

Design, construction and testing of a Pulsejet engine

(versão final após defesa)

Antonio Amezcua Sánchez

Dissertação para obtenção do Grau de Mestre em
Engenharia Aeronáutica
(2º ciclo de estudos)

Orientador: Prof. Doctor Francisco Miguel Ribeiro Proença Brójo

Covilhã, Outubro de 2022

Declaração de Integridade

Eu, ANTONIO AMEZCUA SÁNCHEZ, que abaixo assino, estudante com o número de inscrição 47630 do DEPARTAMENTO DE CIÊNCIAS AEROESPACIAIS da Faculdade DE ENGENHARIA, declaro ter desenvolvido o presente trabalho e elaborado o presente texto em total consonância com o **Código de Integridades da Universidade da Beira Interior**.

Mais concretamente afirmo não ter incorrido em qualquer das variedades de Fraude Académica, e que aqui declaro conhecer, que em particular atendi à exigida referenciação de frases, extratos, imagens e outras formas de trabalho intelectual, e assumindo assim na íntegra as responsabilidades da autoria.

Universidade da Beira Interior, Covilhã 28 /07 /2022

Dedication

To all my family and friends. Especially to my parents and my sister for having been by my side during these four years. Also to my degree and life partner Othman for having made me enjoy this path and not just the finish line.

Acknowledgments

One of the peculiarities that this work has had is that it contains a construction phase in which third parties have been involved. In this way, I wanted to reflect the people who have made it possible. Thus, I would firstly like to thank my tutor, Prof. Doctor Francisco Brójo, for the availability and good work that he has shown throughout the development of the project. Also, to Mr. Pedro Manuel Oliveira who has acted as a laboratory technician, getting personally involved in the preparation of the test bench. Finally, I would like to thank all the staff who collaborate in the maintenance of the propulsive systems laboratory at the UBI.

Abstract

During World War II the pulse jet engine concept was widely used. However, the high level of noise or the excess of vibrations characteristic of this type of engine caused its disappearance from civil aviation. It is true that the low manufacturing cost, the absence of moving parts and its simplicity have increased the interest in entering the unmanned aerial vehicle (UAV) market. Although the origin of the Pulsejet goes back many years, there are many unknowns related to its efficiency and operation in general. Therefore, this thesis aims to design, build and test a valveless Chinese-type Pulsejet engine. The experimental study showed after several tests that the exhaust duct had to be increased by 1/3 of the total length and that the nozzle of this duct was essential to achieve self-sustaining combustion. To draw these conclusions, different tests were carried out, varying the injected fuel flow rate from 1 [g/s] to 4 [g/s]. For each scenario, the following parameters were recorded with the help of a test bench already manufactured in the UBI laboratory: thrust, combustion chamber temperature and sound pressure level. The maximum thrust recorded was 6.72 [N], a value below that stipulated by the literature but consistent with its dimensions. A specific thrust consumption was obtained that was well below the expected theoretical one, for the thrust obtained. This implies and leaves the door open to experiment with much higher flow rates, as it has been shown that self-sustaining combustion remains active.

Keywords

Pulsejet; Valveless Pulsejet; Emissions; Performance; Deflagration; Simplicity.

Resumo

Durante a Segunda Guerra Mundial, o conceito de motor a pulsojato foi amplamente utilizado. No entanto, em alta nível de ruído ou o excesso de vibrações característico deste tipo de motor causou o seu desaparecimento da aviação civil. É verdade que o baixo custo de fabricação, a ausência de peças móveis e sua simplicidade aumentaram o interesse em entrar no mercado de veículos aéreos não tripulados (UAV). Embora a origem do Pulsejet remonte à muitos anos, existem muitas incógnitas relacionado com à sua eficiência e operação em geral. Portanto, esta tese tem como objetivo projetar, construir e testar um motor pulsojato do tipo chinês sem válvulas. O estudo experimental mostrou após vários testes que o duto de exaustão teve que ser aumentado por 1/3 do comprimento total e que o bocal desta conduta foi essencial para alcançar combustão. Para tirar essas conclusões, foram realizados diferentes testes, variando a razão de combustível injetado de 1 [g/s] a 4 [g/s]. Para cada cenário, os seguintes parâmetros foram registados com a ajuda de uma bancada de testes já fabricada no laboratório da UBI: tração, temperatura da câmara de combustão e nível de pressão sonora. A tração máxima registrado foi de 6,72 [N], valor abaixo do estipulado pela literatura, mas compatível com suas dimensões. Obteve-se um consumo específico de tração bem abaixo do teórico esperado, para a tração obtida. Isso implica experimentar com razão de fluxo muito mais altas, pois foi demonstrado que o funcionamento autossustentável permanece ativo.

Palavras-chave

Pulsojato;Pulsojato não valvulado;Emissões;Atuação;Deflagração;Simplicidade.

General Index

List of Figures	xvii
List of Tables	xxi
1 Introduction	1
1.1 Motivation	1
1.2 Goals of the Investigation	2
1.3 Methodology and Structure	2
2 Literature Review	5
2.1 Historic Context	5
2.2 State of the Art	8
3 Theoretical Aspects	13
3.1 Pulsejet	13
3.2 Valved Pulsejet	13
3.3 Valveless Pulsejet	15
3.3.1 Types of Valveless Pulsejet	16
3.4 Pulse Detonation Engine	19
3.5 Operational Cycle	20
3.6 Thermodynamic Cycle	21
3.6.1 Lenoir's Cycle	22
3.6.2 Humphrey's Cycle	22

3.7	Maximum Static Thrust	25
3.8	Frequency of Operation	25
3.9	Starting a Pulsejet	26
3.9.1	Fuel	26
3.9.2	Compressed Air	27
3.9.3	Source of Ignition	27
3.10	Pulsejet relative to other Propulsive Systems	28
3.11	Improving the Performance of a Pulsejet	28
4	Manufacture of the Pulsejet Engine	33
4.1	Initial Pulsejet SetUp	33
4.2	Manufacture of the Pulsejet	34
4.2.1	Admission	34
4.2.2	Combustion Chamber	35
4.2.3	Exhaust	36
4.3	Test Bench	36
4.4	Complementary Systems	37
4.4.1	Ignition System	37
4.4.2	Fuel Injection System	38
4.4.3	Compressed Air System	39
4.5	Operational Problems	39
4.5.1	Ignition	39
4.5.2	Self-Sustaining Pulsing Effect	40
4.5.3	Constant Thrust	40
4.5.4	Fuel	40
4.6	Final Pulsejet SetUp	40
5	Experimental Tests and Results	43

5.1	Data Acquisition Instruments	43
5.1.1	Temperature	43
5.1.2	Thrust	44
5.1.3	Fuel Mass Flow	45
5.1.4	Sound Pressure Level	45
5.2	Experimental Procedure for Data Acquisition	46
5.3	Outcomes	47
5.3.1	Fuel Mass Flow	48
5.3.2	Temperature	48
5.3.3	Thrust	49
5.3.4	Fuel Consumption	51
5.3.5	Frequency	52
5.3.6	Sound Pressure Level	52
6	Conclusions and Future Work	55
6.1	Conclusions	55
6.2	Future Work	56
	Bibliography	63

List of Figures

2.1	V-1 Flying Bomb [1]	6
2.2	Pulsejet Scopette [2]	7
2.3	Pulsejet "U" Shape [5]	7
2.4	Pulsejet sizing and measurement points [3]	9
2.5	Pulsejet pressure and thrust for an intake length of 2.4 [cm] [3]	9
2.6	Velocity vector in the combustion chamber for an external flow of 80 [m/s] with an obstruction. [4]	11
3.1	Flow through a paddle valve [1]	14
3.2	Petal shaved valve [1]	14
3.3	Valveless Pulsejet [5]	15
3.4	Marconnet Pulsejet [3]	16
3.5	Escopette Pulsejet [3]	17
3.6	Lockwood-Hiller Pulsejet [3]	17
3.7	Chinese Pulsejet [3]	18
3.8	Thermojet	18
3.9	Kentifield Pulsejet [6]	18
3.10	Independent use of a PDE [5]	19
3.11	Valveless pulsejet operational cycle [3]	20
3.12	Comparison between Diesel and Otto cycle [3]	21
3.13	Lenoir's ideal cycle [7]	22
3.14	Humphrey's ideal cycle [5]	23

3.15	Intermittent fuel injection mechanism [6]	29
3.16	Conventional intake valve geometry and first mode of vibration [6]	29
3.17	Prototype improvement valve I [6]	30
3.18	Prototype improvement valve II [6]	30
3.19	Thrust augmentator operating principle [3]	31
4.1	Initial dimensions of the Pulsejet	34
4.2	Inlet Ducts	35
4.3	Combustion Chamber	35
4.4	Intake and Exhaust ducts before being manipulated	36
4.5	Pulsejet installed on the test bench [3]	37
4.6	Ignition system [3]	38
4.7	Fuel injection system [3]	39
5.1	Thermocouple installed on the Pulsejet	44
5.2	Load cell fixed to the test bench	44
5.3	Platform for measuring the mass flow rate of fuel	45
5.4	Sound level meter SW-524 [3]	46
5.5	Experimental equipment for data acquisition [3]	47
5.6	Combustion chamber heating	49
5.7	Relationship between thrust and time	49
5.8	Relationship between thrust and fuel mass flow	50
5.9	Maximum thrust value	51
5.10	SW-524	52
5.11	Relationship between sound pressure level and fuel mass flow	53

List of Tables

2.1	V-1 characteristics	6
2.2	Historic aircraft incorporating Pulsejet adapted from [5]	8
5.1	Environmental properties	46
5.2	Fuel Mass Flow	48
5.3	Thrust Specific Fuel Consumption of the Pulsejet	51

List of Symbols

M	Mach Number	[-]
P_a	Ambient Pressure	[Pa]
P_{0a}	Stagnation Ambient Pressure	[Pa]
P_{01}	Stagnation Pressure at the intake	[Pa]
P_{02}	Stagnation Pressure after Compression	[Pa]
P_{03}	Stagnation Pressure after Combustion	[Pa]
P_4	Pressure after Exhaust Duct Nozzle	[Pa]
T_a	Ambient Temperature	[K]
T_{0a}	Stagnation Ambient Temperature	[K]
T_{01}	Stagnation Temperature at the intake	[K]
T_{02}	Stagnation Temperature after Compression	[K]
T_{03}	Stagnation Temperature after Combustion	[K]
T_4	Temperature after Exhaust Duct Nozzle	[K]
\dot{m}_a	Air Mass Flow	[kg/s]
\dot{m}_f	Fuel Mass Flow	[kg/s]
c_{Pc}	Specific Heat at Constant Pressure (cold)	1.005 [kJ/(kg K)]
c_{Ph}	Specific Heat at Constant Pressure (hot)	1.148 [kJ/(kg K)]
Q_R	Fuel Heating Power	46 360 [kJ/kg]
r	Mass Flow Ratio between Air and Fuel	[-]
U	Flight Speed	[m/s]
U_e	Exit Speed	[m/s]
F	Thrust	[N]
$TSFC$	Thrust Specific Fuel Consumption	[kg/(N h)]
L	Pulsejet Length	[m]
L_a	Pulsejet Admission Length	[m]
L_e	Pulsejet Escape Length	[m]
S_a	Transversal Surface of the Admission Duct	[m ²]
V	Total Pulsejet Volume	[m ³]
V_{cc}	Combustion Chamber Pulsejet Volume	[m ³]
f	Pulsejet Frequency	[Hz]
f_a	Pulsejet Admission Frequency	[Hz]
f_e	Pulsejet Escape Frequency	[Hz]
c	Sound Speed	[m/s]
c_a	Admission Sound Speed	[m/s]
c_e	Escape Sound Speed	[m/s]
γ_c	Adiabatic Constant (Cold)	1.400 [-]
γ_h	Adiabatic Constant (Hot)	1.333 [-]
η_d	Admission Efficiency	[-]
η_b	Combustion Efficiency	[-]
Δt	Time Period	[s]
λ	Wave Length	[m]

Chapter 1

Introduction

In this first chapter the foundations of the work will be established. The reason for carrying out this study and the objectives that are intended to be achieved will be cited. Finally, we will talk about the methodology and the structure that has been followed from start to finish.

1.1 Motivation

The development of aviation in general terms is based on the greatest use of energy possible, reducing losses to the maximum. That is why, in the last century, different propulsive systems have appeared to satisfy different needs. These systems coupled to the aircraft have been studied to verify both their range of application and their effectiveness and performance. Among them, we identify four large groups: turbojet, turboprop, propellers (piston-prop) and turbofan.

Parallel to these four groups, during the period of the Second World War, a new concept of jet engine was born that was peculiar in many respects. Pulsejet propulsion can be considered as an intermediate development between piston and gas turbine engines. The main advantage of this type of propulsive system over other engines is based on the partial or total absence (in the case of valveless jet engines) of moving parts. Hence, its design, manufacturing and maintenance costs are very low.

Despite this, this type of engine has not gained a foothold in civil aviation due to the numerous problems that derive from it. Excessive fuel consumption required by this type of engine, high vibrations or noise are some of the causes. However, there is great interest in this type of system in unmanned vehicles; where simplicity as a key element overcomes the previous limitations.

It is true that currently, in the different types of aviation, the eyes are on electric propulsion. Although, the energy storage capacity compromises its range of application. In particular, unmanned vehicles carry out long-range missions where a large size and mass of batteries coupled to the aircraft is required, as their energy and power are still low.

For all these reasons, interest arises in increasing the efficiency of pulsejet propulsion

systems. Modifications in the geometry of the exhaust in order to improve the thrust produced, the amount and type of fuel used, as well as the implementation of lighter materials capable of withstanding high combustion temperatures are some of the goals to be achieved today.

1.2 Goals of the Investigation

This document corresponds to a final degree project carried out at the University of Beira Interior. The pillars of the research are explained below.

In the first place, we proceed to study the theoretical foundations of a Pulsejet engine. Thus encompassing the different morphologies of pulse jet propulsion systems. Understand in depth the principles that this type of motor follows and the parameters on which it depends. This includes the study of the different stages of combustion as well as the related thermodynamic cycles. The second part of the work will have as its purpose the design and construction of a previously designed valveless pulsejet engine prototype with the possibility of modifying certain geometries (such as the exhaust or the intake itself). It is worth mentioning that this part will be subject to the availability of material and technology from the UBI aeronautical engineering department.

Finally, the prototype will be submitted to a static test bench where experimental data will be obtained to later compare them with the theoretical or ideal values. The ignition and injection systems will be modified in order to contrast and obtain relevant conclusions about this propulsion system. To do this, sensors incorporated in the test bench will be used to record the operating parameters.

During the development of the memory, the problems encountered will be detailed and the appropriate conclusions will be mentioned in order to help and speed up the possible future investigation of pulse jet systems.

1.3 Methodology and Structure

In order to structure and achieve the best possible understanding of this end-of-degree project, the memory has been divided into six well-differentiated chapters.

The first of them contextualizes the objectives to be achieved with the present work as well as the organization that has been carried out. It also highlights the existing motivation to deal with the topic in question.

A second chapter is available in which the historical trajectory of pulse jet propulsive systems is evaluated. In it, graphic examples of its evolution and the different modifications made until reaching the Pulsejet engine that we know today are shown.

The third point is based on the theoretical foundations of the behavior of a Pulsejet. Each of the most relevant operating parameters will be analyzed; calculating some of them to contrast values with point five of the work.

Furthermore, the fourth and fifth points can be considered to go hand in hand. Firstly, the design and construction of the valveless engine is carried out with the help of the coordinator of this project. Next, it is detailed in depth how the test bench that will be used should be and the sensors that must be incorporated in it to obtain data, as well as an analysis of results and their discussion is introduced.

Finally, in point six of the report, the conclusions obtained and the problems encountered in carrying out the tests are presented. A general assessment of the objectives set at the beginning of the project is also carried out and new research horizons are opened for future related work.

Chapter 2

Literature Review

Since the first model of a Pulsejet engine was developed, dating back to the early 20th century, efficiency and performance improvements have been made. Next, the different stages and investigations that this type of engine has undergone over the years will be cited.

2.1 Historic Context

It is difficult to select a single inventor of the Pulsejet engine as its history is quite confusing. The title can be divided between two people at the beginning of the 20th century: the Russian officer Nikolaj Teleshov and the Swedish inventor Martin Wiberg.

Although, the first known official patent occurred in 1906 and is attributed to another Russian engineer named V.V Karadovin [8]. It was a high-frequency engine using the cyclic combustion of a mixture of liquid fuel and air.

It was in 1906 in France that George Macconet invented the first primitive valveless pulse jet model [9]. This was formed by an inlet diffuser connected to a combustion chamber followed by an exhaust nozzle to expel the gases derived from combustion.

The first attempt to use this type of engine in an aircraft was made by the German designer Paul Schmidt in 1939. It was the "V-1 flying bomb" (see *Figure 2.1*). The first model incorporated the engine inside the fuselage. Initially it was denied by the German Air Force Ministry on the grounds of a reduced operating range and high cost.



Figure 2.1: V-1 Flying Bomb [1]

Based on Schmidt’s model, the German company Argus Company perfected the Pulsejet, obtaining flight approval in December 1942. The model was an unmanned bomb similar to a missile, weighing more than two tons, which had as a method of guidance a gyroscope. When the fuel on board ran out, it crashed to the ground. The characteristics of the V-1 are reflected in *Table 2.1*.

Table 2.1: V-1 characteristics

Thrust	Flight Altitude	Cruise Speed	Launch Pad
2900 [N]	1000 [m]	640 [km/h]	- Inclined ramp of 46 [m] - Launch Plane

The V-1 had an important participation in the bombings of the second world war that occurred in Belgium and England. It is considered the first widely used cruise missile. [1]

In the last years of the war, the American army recovers remains of the V-1 and builds its own cruise missile, the Jet Bomb 2. With the help of the USAAF, they manage to develop a missile equipped with a PJ-31 Pulsejet engine. Produced by Ford. It was very similar to the V-1 in having the same launch pads. The United States also uses the Marconnet Pulsejet as its starting model and gives rise to the “Resojet”. The main difference was the sudden acceleration of the flow that occurred at the entrance of the combustion chamber; allowing a significant improvement in combustion efficiency as the air/fuel mixture is produced faster.

In the same year, the opposing side formed by the Japanese, created the Yokosuka MXY7 based on a Pulsejet engine intended for the creation of aircraft guided by pilots in order

to carry out suicide attacks.

A team of engineers belonging to the SNECMA company created the first valveless jet engine in 1950. It was called “Scopette” and its peculiarity was found in the admission as it was turned backwards (see *Figure 2.2*). This produced an increase in the thrust when the flow reversal effect occurred [2]. Another feature to mention is found in the propelling nozzle. It was not a straight tube with a constant section, but rather different diameters differentiating stages in the exhaust and favoring the production of compression waves.



Figure 2.2: Pulsejet Scopette [2]

The prototype that is most similar to the Pulsejet that we know today was developed in the early 1960s by Lockwood together with the Hiller company. A “U”-shaped pulse jet that had a variable area geometry throughout its structure, as seen in *Figure 2.3*. It was made up of a shorter intake tube and a curved nozzle for the combustion gases. It is considered one of the most effective models as it allows the installation of servomotors both in the intake and in the exhaust, considerably increasing the performance of the engine. This was capable of producing a maximum thrust of 1335 [N] with a mass of around 15 [kg]. [6]



Figure 2.3: Pulsejet "U" Shape [5]

In the following two decades it is worth mentioning the technological advance discovered by John Kentfield; the addition of a structure called a recuperator. A slightly curved cone that produced a regeneration of fresh air in the secondary cycle, improving it. The problem of having a jet engine with intermittent operation when drawing in fresh air led Kentfield to decide on a lateral air regeneration where the air was more easily accelerated.

The most recent use of the Pulsejet engine was by the American manufacturer Boeing. The technology called PETA incorporates these Pulsejet propulsion systems into vertical takeoff and landing (VTOL) aircraft. The idea is to insert a Pulsejet engine into a duct. As the air flow is released by the exhaust nozzle, an air entrainment is produced which, on the one hand, cools the engine quickly and, on the other hand, increases the thrust. Research

underway by Boeing and NASA seeks to incorporate this technology into LAMVs: vertical takeoff and landing aircraft. [2]

As a summary, *Table 2.2* compiles the different aircraft along with their operating parameters that have incorporated Pulsejet engines throughout the most recent history.

Table 2.2: Historic aircraft incorporating Pulsejet adapted from [5]

Characteristic	XH-26 Jet Speed	ARSAERO CT10	Curtiss KD2C Skeet	Kawanishi Baika
MTOW	320 [kg]	660 [kg]	571 [kg]	750 [kg]
Maximum Speed	175 [km/h]	420 [km/h]	539 [km/h]	649 [km/h]
First Flight	1952	1951	1947	1944
Mision	Observation and reconnaissance	Bomber	Drone	Suicide Aircraft
Field	Military	Military	Military	Military

2.2 State of the Art

It is true that interest in the Pulsejet engine has decreased compared to the research carried out in the 20th century. Although, its ease and low cost of production have led to studies being taken up again in order to improve its performance and even implement it in certain types of aircraft, as has been said previously.

Scientists Tao and Wenxiang et al. [10] carried out a numerical study on a valveless Pulsejet and came to the conclusions that the air-fuel mixture is ignited by the products of combustion at high temperatures, produced in the previous combustion cycle. It is precisely this that causes the self-sustainability of the pulsating effect. The second conclusion referred to the depletion of exhaust gases, which cause a suction process responsible for admitting air into the combustion chamber; giving rise to a new operating cycle.

Paxson [11] wanted to know how thrust could be improved and what would be the optimal sizing of the Pulsejet mass flow. After using different ejectors with variable geometries, he concluded that what most favors the increase in thrust is not its radius, but rather placing it close to the exhaust duct. Furthermore, it was shown that mass flow and thrust are not closely related.

On the other hand, Wenxiang et al. [10], investigated how the variation in the length of the propelling nozzle and the combustion chamber compromise the performance of a pulse jet engine. To do this, they did a numerical simulation with CFD (CFXTM 11.0), to a Chinese-type valveless pulse jet of 830 [mm] length fueled with propane gas with a constant mass flow rate of 0.4 [g/s]. The simulations carried out allowed them to conclude that the frequency of the pulsejet increases with the decrease in the length of the combustion chamber and, on the other hand, there is a characteristic length capable of minimizing the frequency for the case of the outlet duct. Furthermore, they testified that a decrease in chamber length of more than 30mm causes a sudden increase in thruster frequency.

Geng [4] conducted one of the most detailed experiments to date. In it, temperature,

operating frequency, pressure and thrust were measured by making variations in the length and geometry of the exhaust and intake ducts. The pulsejet sizing and measurement points are visible in *Figure 2.4*.

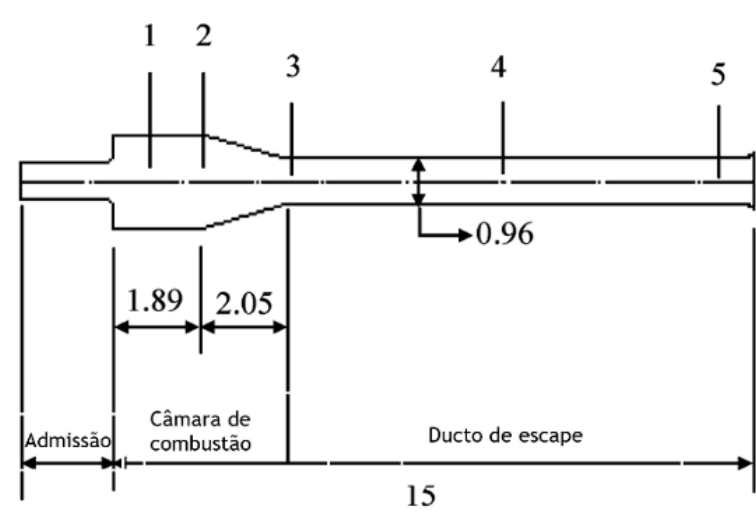


Figure 2.4: Pulsejet sizing and measurement points [3]

Figure 2.5 reflects the sinusoidal trend of the pressure measured at point 2 (see *Figure 2.4*) and the thrust value as a function of time, being this second one measured with the help of a load cell.

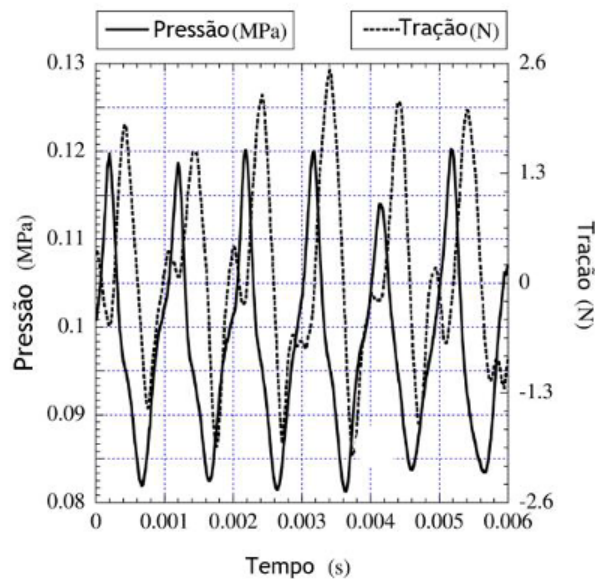


Figure 2.5: Pulsejet pressure and thrust for an intake length of 2.4 [cm] [3]

The main conclusion was to realize the close relationship between the intake and exhaust ducts. A reduction in the overall length of the engine implies modifying the intake duct to maintain self-sustaining combustion. Regarding the frequency of the valveless propellant, it was shown that this decreases with an increase in the total length of the motor. It is worth mentioning that Geng [4] used the following orientations for the intake duct: 90° , 135° and 180° . In all of them the pulsating effect was achieved and it was verified that the fuel injection was facilitated the greater the angle in the elbow of the intake duct.

In the experiment, the fuel used, since it was a scale model, was hydrogen. The relationship between the fuel flow with the maximum pressure and the operating frequency was confirmed. For low flow rates, these parameters are reduced, increasing progressively as the flow rate increases.

It is relevant to know how the motor acts under certain flight conditions. To do this, Nakano [12] entered a 80cm valveless Pulsejet with a 3.4cm gas-powered duct into a wind tunnel. The results revealed that as flight speed increases, thrust decreases. This occurs because as the flight speed increases, the incident air flow in the intake duct also increases, which generates an excess of oxygen in combustion. That is, by introducing an air flow control system in the intake, a fuel reduction of 20 % was achieved.

The way in which the operating frequency of a valveless Pulsejet can be measured was also studied. Zheng et al. [4] implemented an acoustic model that showed that the frequency depended on the average speed of sound (a function of temperature) and the geometry of the nozzle inlet. The modus operandi of the system consisted of the average of the frequencies in the intake and exhaust ducts. If these are equal, the maximum thrust value is obtained. However, if the difference between the two exceeds a critical value, the Pulsejet stops working. At the same time, an increase in the diameter of the intake duct implies a reduction in the inlet temperature.

Based on studies by Nakano et al. [12], Zheng confirmed that a valveless Pulsejet engine in the presence of high-velocity external airflow is capable of drawing air directly from the inlet to the propellant nozzle, passing through the combustion chamber without this having any participation in the combustion. Hence, the need arises to create vorticity in the combustion chamber in order to favor the mixing of the internal flow. An obstruction was placed inside it (see *Figure 2.6*) and a slight increase in thrust was seen and the frequency values in the intake and exhaust ducts remained constant. Similarly, the static case was carried out and it was concluded that the addition of a disturbance in the combustion chamber did not cause significant changes in pressure and thrust.

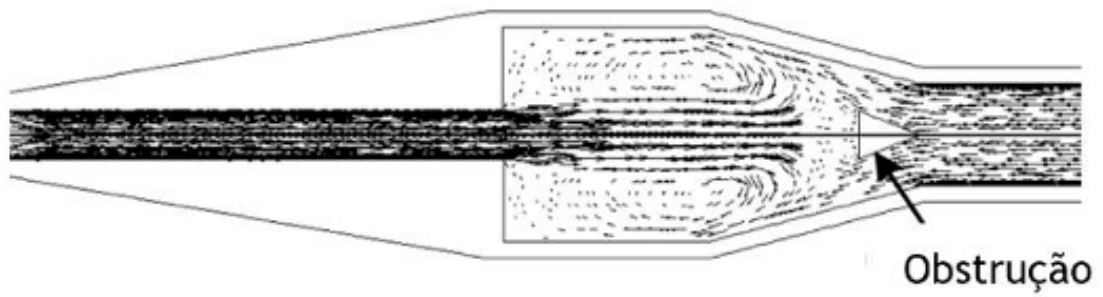


Figure 2.6: Velocity vector in the combustion chamber for an external flow of 80 [m/s] with an obstruction. [4]

Chapter 3

Theoretical Aspects

In order to understand the operation of a Pulsejet propulsion system, it is necessary to delve into some relevant concepts and definitions. That is why, during this chapter, the physical and thermodynamic principles of a Pulsejet engine, the different stages of operation will be collected and it will end by citing procedures capable of improving its performance.

3.1 Pulsejet

As has already been said in previous chapters, the Pulsejet can be considered as an intermediate development between piston engines (intermittent combustion cycle of the air-fuel mixture) and gas turbines (continuous). There are similarities also with ramjet engines; Linear path of the mixture from the intake to the exhaust or the emission of gases at high temperatures with the aim of generating thrust in the exhaust.

In general terms, it can be considered as a simple configuration engine. Thus, finding different typologies that even lack moving parts. The basic structure is formed by an intake or air intake followed immediately by the combustion chamber and a resonant exhaust with the possibility of adding an outlet nozzle to increase thrust. The most peculiar characteristic of this type of engine is the generation of intermittent thrust. This occurs due to an intermittent admission that generates pulsating combustion. Next, the three existing types of pulse jet will be developed: with valves, without valves and with a pulse detonation engine. [3]

3.2 Valved Pulsejet

The installation of valves in the intake prevents the combustion products from refluxing during the combustion process. In other words, this mechanical system made up of unidirectional or retention valves allow the suction of the air, driving it directly to the combustion chamber, avoiding the exit of air in the intake. The most used type of valve is the grid system with paddle valves that open and close when they detect changes in pressure on the opposite side of the valve (See *Figure 3.1*).

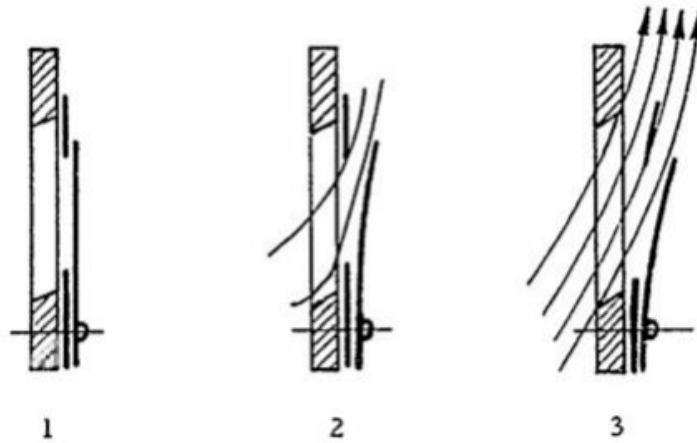


Figure 3.1: Flow through a paddle valve [1]

The fuel, which can be a gas or aerosol, is mixed with the incoming air at the intake or it is injected directly into the combustion chamber. Once the mixture is formed, the spark is triggered, causing the valves to close automatically upon detecting a considerable increase in pressure inside the combustion chamber. Thus, it is achieved that the hot gases from combustion have a single exit, the exhaust. The generation of thrust can be explained with the action-reaction principle (Newton's third law). When the gases are expelled, a pressure lower than atmospheric pressure is perceived in the combustion chamber, causing the opening of the valves and thus the regeneration of air in the intake for the repetition of the cycle. There are other types of valves that are used in the smaller models that have a petal shape. They are made up of a perforated ring and a disk with the same shape that covers each of the holes (See *Figure 3.2*).

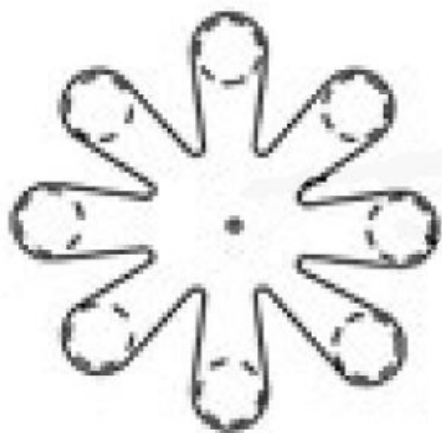


Figure 3.2: Petal shaped valve [1]

However, the biggest problem with any type of valve is the operating life of the valve.

The continuous exposure to cycles of overpressure during the explosion of the mixture in the combustion chamber affects their durability. The same is true for petal valves. These are also affected by the very high temperatures of the combustion chamber that generate cracks and deformations in the steel disc. That is why most studies focus on increasing the operating range of the valves by installing a cooling system [13]. As a future development, it would be quite interesting to be able to control the flow in the intake of the combustion chamber.

3.3 Valveless Pulsejet

The durability of valve systems is a problem that continues to this day and entails high maintenance and repair costs. Therefore, the need arises to create the pulsejet with the absence of moving parts in the intake. Although the geometry of the Pulsejet itself has aerodynamic valves that restrict the flow of gases in one direction, thus preventing the reflux of gases derived from combustion. The common anatomy of all types of valveless Pulsejet systems consists of a combustion chamber with attached ducts. Normally, the shortest duct corresponds to the intake and the longest to the exhaust. The main characteristic is based on the fact that when the burned air-fuel mixture expands, the gases at high temperature are expelled both through the exhaust duct and through the intake duct. This is the main difference with engines with valves that control said reflux at all times.

The direct consequence of both ducts functioning as exhaust is that they must be placed in the same direction. Otherwise, the thrust obtained would be highly damaged as each conduit would partially cancel each other out (See *Figure 3.3*). Therefore, as will be detailed in the next section, most designs without valves take this detail into account.

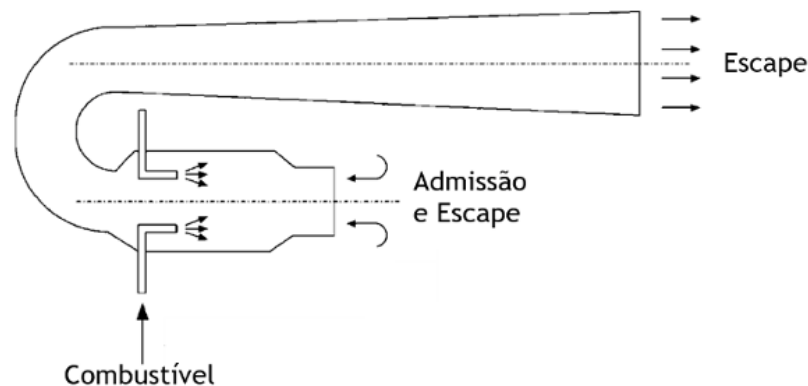


Figure 3.3: Valveless Pulsejet [5]

From the point of view of efficiency, it is necessary to analyze the wavefronts produced after combustion in both ducts. It has been shown that maximum thrust is obtained when the intake and exhaust frequencies match. Thus, a stable combustion is achieved that favors thrust.

Compared to valve engines, valveless Pulsejets require a larger size to achieve the same thrust. The efficiency of the latter is lower than when there are valves; there is a depletion of the hot gases during the expansion stage in both ducts, causing a lower internal pressure as the air is not regenerated as quickly.

Although, it must be said that the extreme ease of its construction is a notable advantage over valve propulsion systems. Only the welding of steel tubes and cones are sufficient for its manufacture.

3.3.1 Types of Valveless Pulsejet

There are different types of valveless Pulsejet engines depending on the size of the intake and exhaust ducts. The size of the impeller will determine the fuel to choose in order to achieve self-sustained combustion. The different types present are listed below.

First of all, it is necessary to talk about one of the oldest configurations, developed 100 years ago by Georges Marconnet (See *Figure 3.4*). It is a Pulsejet without valves that causes the gases derived from combustion to be expelled through the intake and exhaust pipes, generating irregularities in the thrust.

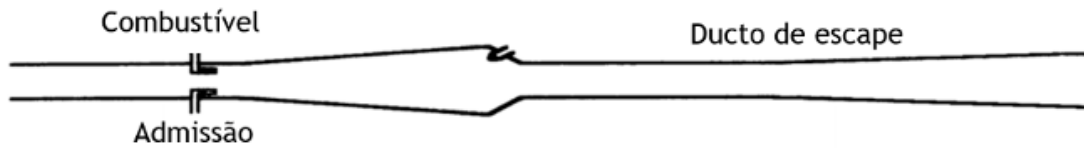


Figure 3.4: Marconnet Pulsejet [3]

We can say that the Escopette is an evolution of the model proposed by Marconnet. A change of direction in the intake duct (*Figure 3.5*) allows the exhaust gases to flow in the same direction, bypassing the asymmetry in thrust and increasing said thrust as well. In addition, there is a space between the U-shaped duct and the intake that allows air regeneration for the next work cycle.

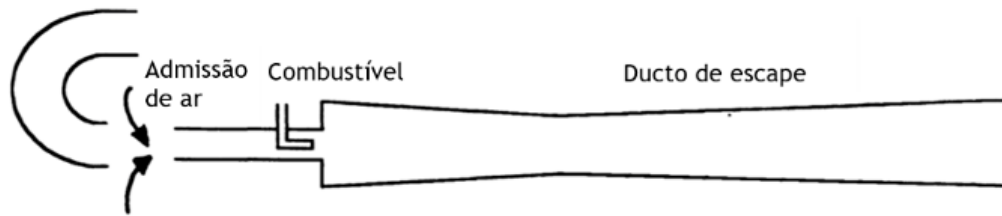


Figure 3.5: Escopette Pulsejet [3]

The main difference between the Scopette and the Lockwood-Hiller model is the coupling of thrust augmentators in the inlet and outlet ducts (*Figure 3.6*). With this, it is possible to increase the thrust considerably by producing an expansion of the inlet air, as will be detailed in section 3.11 of this work.

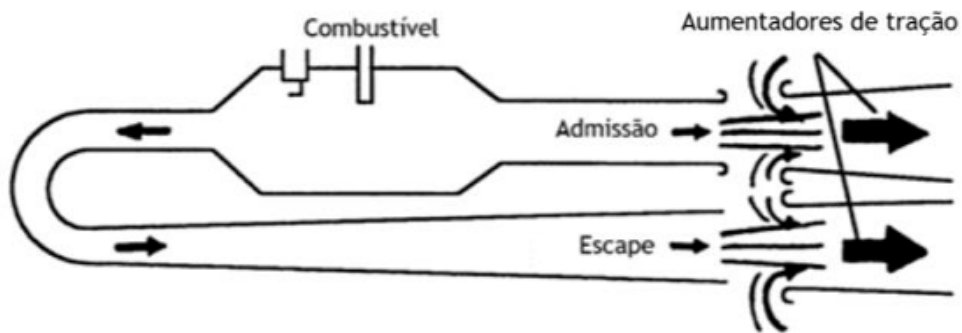


Figure 3.6: Lockwood-Hiller Pulsejet [3]

Another type is the Chinese Pulsejet; It consists of a short intake duct compared to the exhaust duct. Both ducts are oriented in the same direction (*Figure 3.7*).

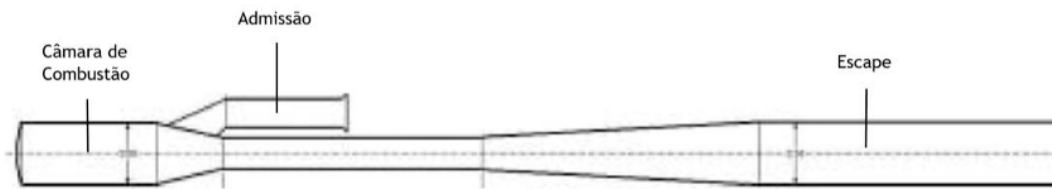


Figure 3.7: Chinese Pulsejet [3]

Analogous to the Chinese Pulsejet, the Thermojet was developed. Two to four intakes parallel to the propelling nozzle make it up (*Figure 3.8*).

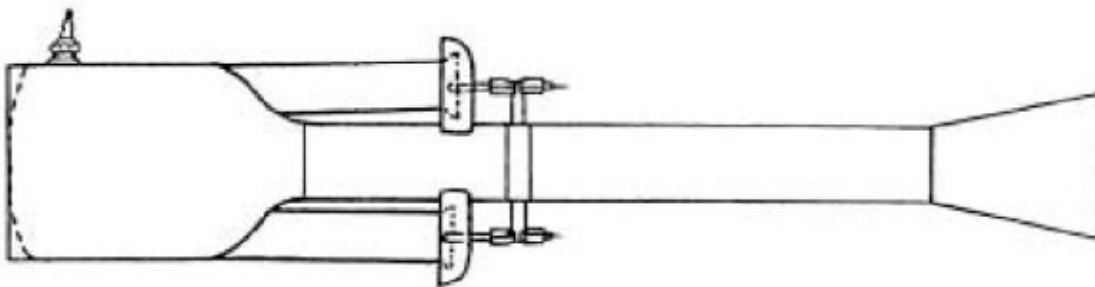


Figure 3.8: Thermojet

Scientist Kentifield [11] developed the most efficient Pulsejet engine model to date. Greater power per length unit and better specific consumption compared to the configurations mentioned above (*Figure 3.9*)

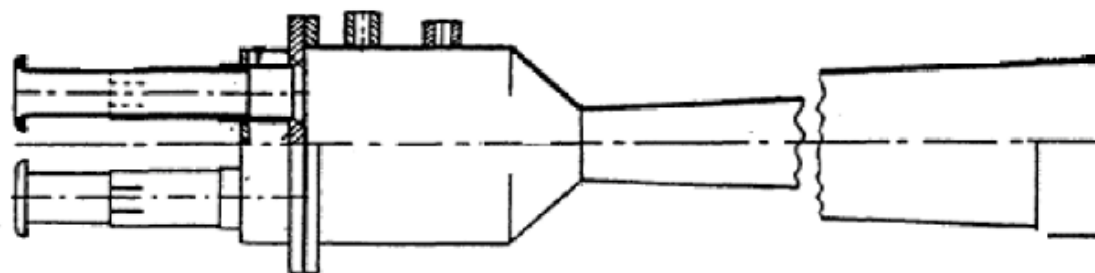


Figure 3.9: Kentifield Pulsejet [6]

3.4 Pulse Detonation Engine

The pulsed detonation engine or PDE is a relative approach to intermittent combustion jet engines. To date, no engine with these characteristics has been marketed. However, companies such as General Electric or Pratt & Whitney are carrying out research for its implementation in the future. Its many advantages include lower manufacturing costs, reduced weight, and more efficient fuel consumption than many Turbofan engines.

Pulsejets developed to date operate in a fuel deflagration regime. That is, rapid combustion occurs but the speed of sound cannot be reached. On the contrary, a new concept of pulse detonation engine which combustion is supersonic is being studied. In other words, while Pulsejets with or without conventional valves deflagrate fuel, PDEs detonate it. These produce an extremely high pressure that translates into an increase in thrust. PDEs can be considered to perform constant volume combustion while Pulsejets with or without valves approach characteristic constant volume combustion. Consequently, it makes PDE engines thermodynamically more efficient despite the fact that some studies reveal the possibility that there are changes in the properties of the thermodynamic state, due to detonation. [14]

Among the applications of PDEs are high-speed passenger transport, space propulsion, military air transport or long-range missiles. All of them require a high specific impulse combined with the efficiency typical of this type of engine.

The form of application of the PDE can vary, being this independent, in a combination of cycles or in a hybrid system. The first is made up solely of an intake, a set of detonation ducts and an outlet nozzle (*Figure 3.10*). The noise problem and the drop in efficiency for high Mach numbers limit its application. When speaking of a cycle combination, it refers to the addition of a PDE to the flow of a ramjet or other jet engine, allowing greater efficiency at higher speeds. Finally, the hybrid system can be interpreted in two ways: replacing the combustion chamber with the PDE or adding it to the bypass of a turbofan so that it is accelerated.

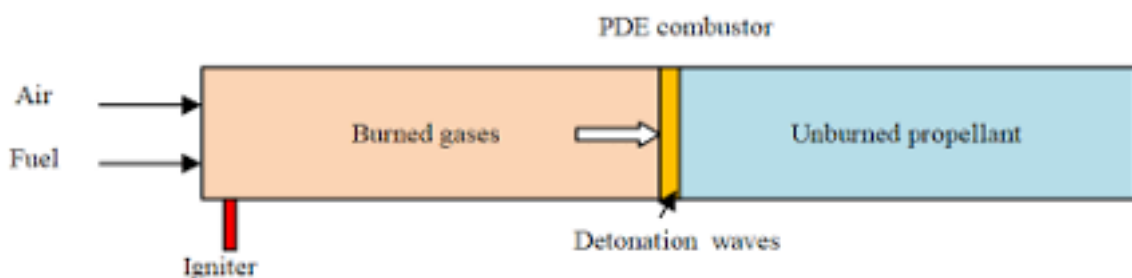


Figure 3.10: Independent use of a PDE [5]

3.5 Operational Cycle

To explain the operational cycle of a valveless Pulsejet engine, the attached image composed of four different stages will be used (*Figure 3.11*).

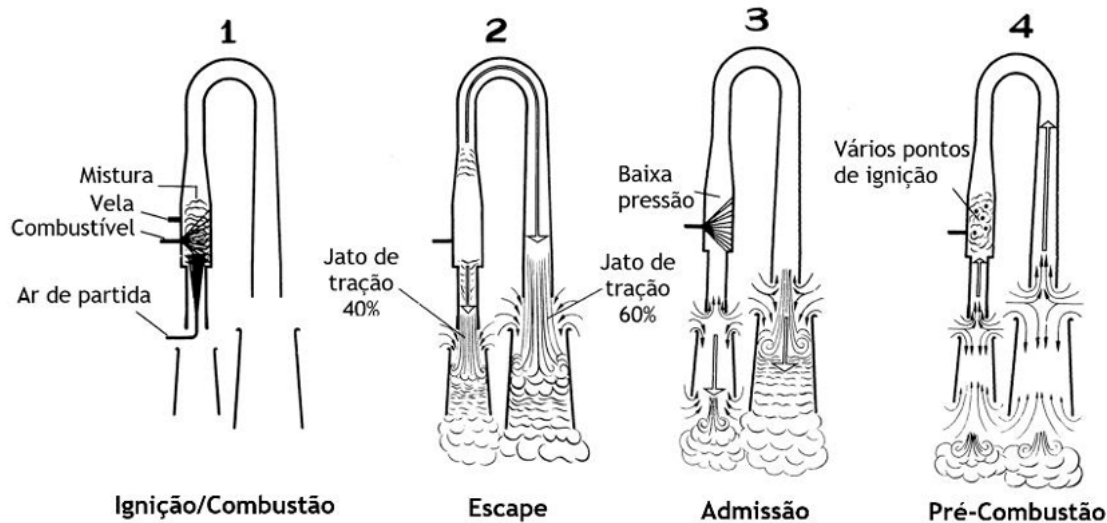


Figure 3.11: Valveless pulsejet operational cycle [3]

In the initial phase (first drawing), the stoichiometric mixture of air and fuel is available and is ignited by a spark, releasing gases such as carbon dioxide and water vapor after combustion. In this stage, the gases increase the pressure of the combustion chamber to its maximum value by occupying a large portion of the interior space, increasing its temperature.

In the second phase (second drawing) the exhaust is represented. In it, the fuel injection is stopped momentarily when there is a high pressure in the combustion chamber. Combustion-derived gases exit through both ducts, contributing to the thrust of the Pulsejet. Since the intake duct is shorter than the exhaust duct, the gases take less time to evacuate than those expelled through the exhaust duct. In this way, under the same pressure in the chamber, the intake duct is free of combustion products while they remain in the exhaust when the intake phase begins.

The third stage is known as admission (third drawing). After the release of the exhaust gases, the pressure in the combustion chamber reaches its minimum value. A partial vacuum is produced in it as gases move from areas of higher pressure to those of lower pressure. Consequently, this pressure difference between the chamber and atmospheric pressure produces the suction of fresh air. In this way, the valveless Pulsejet is able to admit air through the expansion of exhaust gases (Kadenacy effect).

The fourth drawing corresponds to the precombustion stage. At this point no external ignition agent is necessary to ignite the air-fuel mixture. Ignition occurs at several points

due to hot residual gases remaining in the exhaust nozzle. As said before, these are sucked from the exhaust duct into the chamber at the same time as a new charge of air and fuel. The fact of having a multipoint ignition speeds up the combustion time. In this way, it closely approximates constant volume combustion by not allowing the charge to expand until it is completely consumed. It also favors the compression and subsequent ignition due to the rapid recoil of the column of hot gases from the exhaust duct, acting similar to a mechanical piston from an alternative engine.

3.6 Thermodynamic Cycle

To explain the operation of any motor it is necessary to pay attention to the thermodynamic cycle that governs its cycle of operation. While reciprocating engines are normally described by Otto or Diesel cycles, gas turbine engines follow the Brayton cycle. Despite this, the different phases that make up these cycles are common in all cases; air intake, compression and mixing, combustion of the mixture and expulsion of hot gases. The Otto and Diesel cycles are represented below, relating volume-pressure on the one hand and temperature-entropy on the other (*Figure 3.12*).

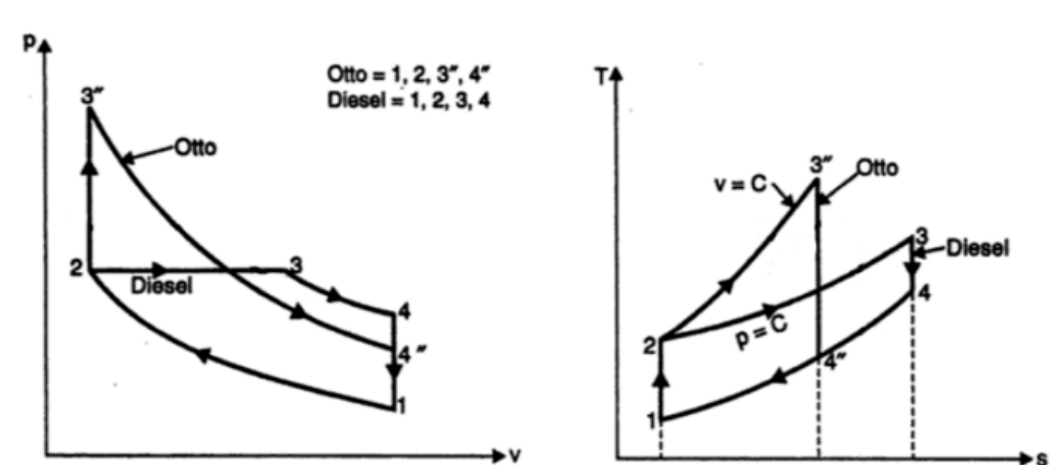


Figure 3.12: Comparison between Diesel and Otto cycle [3]

As seen in both cycles they follow a common structure composed of four processes: 4->1 represents admission, 1->2 compression, 2->3 combustion and 3->4 expansion.

As it will be explained in the next section, the best approximations of the thermodynamic cycle of a Pulsejet engine are the Lenoir cycle and the Humphrey cycle [7]. In the first of these, heat is added at constant volume during combustion and the expansion is isentropic and adiabatic. The Humphrey cycle is similar by adding isentropic compression.

3.6.1 Lenoir's Cycle

In the *Figure 3.13* a representation of the ideal Lenoir cycle is visible relating the following parameters: pressure-volume and temperature-entropy. In it, 1->2 refers to isochoric combustion, 2->3 isentropic expansion without heat exchange with the outside and finally, 3->1 represents isobaric heat rejection. In addition, it is important to add that in the last of the stages, of 3->1, two physical processes occur simultaneously: the admission and the subsequent ignition of the air-fuel mixture.

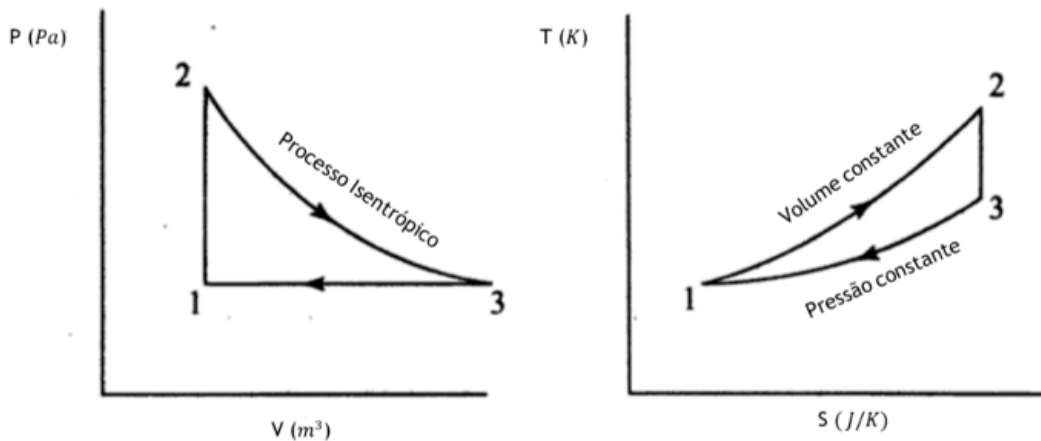


Figure 3.13: Lenoir's ideal cycle [7]

The first of the stages of the Lenoir cycle corresponds to admission (3->1 in the drawing). Here, the combustion chamber is fed by a charge of fresh air. During the next stage, 1->2, the air-fuel mixture is ignited thanks to the hot gases trapped from the previous cycle. Therefore, there is an isochoric combustion where the pressure, temperature and entropy increase notably. The last of the stages of 2->3 corresponds to the isentropic expansion where the combustion products go out both through the intake duct and through the outlet nozzle, generating the desired thrust. Thus, the minimum pressure value in the combustion chamber is reached and the cycle is repeated with a new charge of air and fuel.

3.6.2 Humphrey's Cycle

Parallel to the Lenoir cycle, the *Figure 3.14* represents the ideal Humphrey cycle that closely approximates the thermodynamic behavior of a Pulsejet engine. This thermodynamics cycle only differs from the Otto cycle in the admission process. Unlike the Lenoir cycle, one more stage of compression is added before combustion. In summary, four stages are differentiated: from a->2 an isentropic compression, from 2->3 isochoric combustion, from 3->4 the isentropic expansion of the exhaust gases and finally, from 4->a represents isobaric heat rejection.

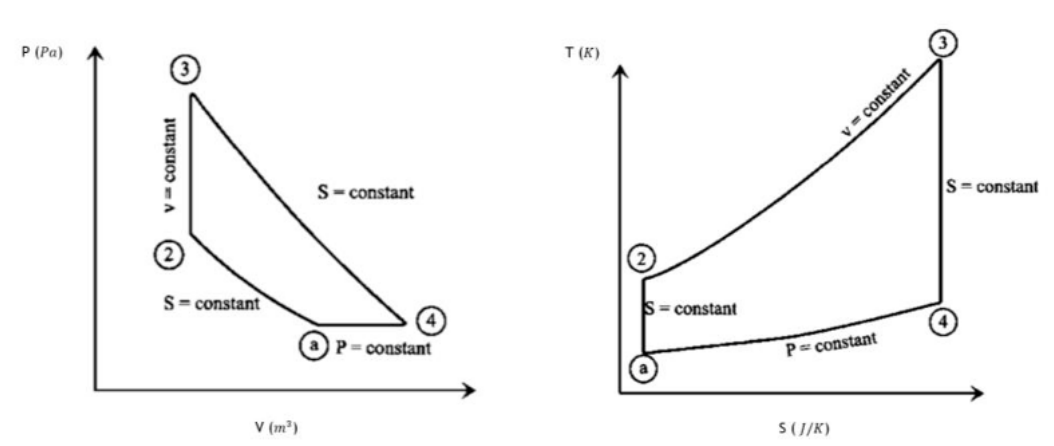


Figure 3.14: Humphrey's ideal cycle [5]

It is necessary to delve into each of the components that make up a Pulsejet engine and carry out the necessary calculations for its correct thermodynamic understanding. Therefore, the most relevant aspects of each of them will be cited below:

- **Inlet Duct**

During the admission process of $a \rightarrow 2$ an intermediate process is distinguished. The state at point (a) corresponds to a free point of air away from the inlet, without flow disturbances. The intermediate point, which is referred to as (1) although it is not shown in the diagram, is located at the entrance on the outside while point (2) is also located at the entrance but on the inside of the engine. An increase in pressure and temperature is experienced from ambient conditions (a) to state conditions (1). The stagnation temperatures and pressures are such that:

$$P_{01} = P_{0a} = P_a \left(1 + \frac{\gamma_c - 1}{2} M^2 \right)^{\frac{\gamma_c}{\gamma_c - 1}} \quad (3.1)$$

$$T_{01} = T_{0a} = T_a \left(1 + \frac{\gamma_c - 1}{2} M^2 \right) \quad (3.2)$$

Due to the losses of the intake duct, the stagnation pressure in (1) differs from the pressure in (2), despite the fact that their stagnation temperatures do coincide ($T_{01} = T_{02}$). Therefore, the stagnation pressure at point (2) will be:

$$P_{02} = P_a \left(1 + \eta_d \frac{\gamma_c - 1}{2} M^2 \right)^{\frac{\gamma_c}{\gamma_c - 1}} \quad (3.3)$$

Note that the symbols that are shown in this equation and the following ones are already defined in the *List of Symbols*, which can be seen at the beginning of the document.

- **Combustion Chamber**

As we have seen before, we can approximate the combustion (2->3) to an isochoric process. In this stage, the maximum value of pressure and temperature is reached when the ignition and subsequent burning of the air-fuel mixture take place. This pressure will be:

$$P_{03} = P_{02} \left(\frac{T_{03}}{T_{02}} \right) \quad (3.4)$$

To obtain the maximum temperature of the cycle that occurs at point (3), it is necessary to carry out an energy balance in the combustion chamber:

$$(\dot{m}_a + \dot{m}_f) c_{Ph} T_{03} = \dot{m}_a c_{Pc} T_{02} + \eta_b \dot{m}_f Q_R \quad (3.5)$$

Note that the value of η_b corresponds to the combustion efficiency and its value depends on the case of study.

From the previous expression, the air-fuel ratio is obtained directly:

$$r_{c/a} = \frac{c_{Ph} T_{03} - c_{Pc} T_{02}}{\eta_b Q_R - c_{Ph} T_{03}} \quad (3.6)$$

- **Exhaust Duct Nozzle**

After combustion, the derived gases are expelled through this conduit and their isentropic expansion occurs until they reach atmospheric pressure. As it is a subsonic combustion, the speed of sound is not reached by the fluid and $P_4 = P_a$ is maintained. The exhaust gas temperature can be obtained with the following relationship:

$$\left(\frac{T_{03}}{T_4} \right) = \left(\frac{P_{03}}{P_a} \right)^{\frac{\gamma_h - 1}{\gamma_h}} \quad (3.7)$$

Also, it is relevant to quantify the escape velocity. The module and the thrust generated are calculated as follows:

$$|\vec{U}_e| = \sqrt{2 C_{Ph} T_{03} \left[1 - \left(\frac{P_a}{P_{03}} \right)^{\frac{\gamma_h - 1}{\gamma_h}} \right]} \quad (3.8)$$

$$|\vec{F}| = \dot{m}_a \left[(1 + r_{c/a}) U_e - U \right] \quad (3.9)$$

The values of U_e and U are defined in the *List of Symbols* and their values are case dependent.

Thrust Specific Fuel Consumption (TSFC) can be calculated as follows:

$$TSFC = \frac{\dot{m}_f}{F} = \frac{r_{c/a}}{F} \frac{\dot{m}_a}{\dot{m}_a} \quad (3.10)$$

3.7 Maximum Static Thrust

This parameter has quantitative magnitudes and can be expressed as a vector. It represents the thrust force capable of propelling the aircraft forward. It comes from pushing a certain mass of gas in the opposite direction to the advance of the aircraft. This air thrust comes from the gases derived from the combustion process.

It is true that in the previous section an approximation was made to calculate the specific thrust. However, it is necessary to know the value of the thrust \vec{F} , which was very difficult to calculate since several iterations were needed to be done.

The studies carried out by the scientist Tharratt [15] seek an alternative solution that does not imply the need to know these two parameters. It is a relationship that is capable of estimating the power module through a relationship between volume and length of the motor. In other words, it is not necessary to know the thermodynamic behavior or the dynamics of the gases inside the combustion chamber.

$$\frac{V}{L} = 6.6 \cdot e^{-5} |\vec{F}| \quad (3.11)$$

Despite the fact that Tharratt's studies correspond to mechanically valved exhaust ducts, they continue to be the only possible solution to calculate the thrust intensity of Pulsejets without valves.

3.8 Frequency of Operation

As with piston engines, the number of cycles per minute is commonly used to describe Pulsejet behavior. The frequency of cycles practiced per second allows to see the speed of work of the jet engines. As there are many types of Pulsejet propelled systems, there is no base expression to predict the frequency of operation. Although, it has been shown that the frequency of the Pulsejet with or without valves is inversely proportional to its total length. Namely:

$$f \propto \frac{1}{L} \quad (3.12)$$

In the case of Pulsejet engines with mechanical valves, there is a parallel reasoning for determining the frequency of operation. $\frac{1}{4}$ wave acoustic terminology divides Pulsejet operation into a system of three pressure waves: compression, rarefaction, second rarefaction, compression. By having operating speeds close to that of sound and a wavelength for each cycle equal to $4L$, the operating frequency can be calculated using the following expression:

$$f = \frac{1}{\Delta t_{cycle}} \approx \frac{1}{\gamma} \approx \frac{c}{4L} \quad (3.13)$$

Valveless pulsejets, on the other hand, follow a theory jointly proposed by Zheng et al and Ordon [4]. These suggest calculating the operating frequency treating the intake as a Helmholtz resonator and the exhaust with the 1/6 wave acoustic theory. Thus, two equations are obtained for the intake and exhaust frequency respectively:

$$f_a = \frac{c_a}{2\pi} \sqrt{\frac{S_a}{V_{cc}L_a}} \quad (3.14)$$

$$f_e = \frac{c_e}{6 L_e} \quad (3.15)$$

Finally, the total operating frequency of the valveless Pulsejet is given by the average of the two frequencies calculated above:

$$f = \frac{f_a + f_e}{2} \quad (3.16)$$

The parameters shown in the previous equations are already defined in *List of Symbols*.

3.9 Starting a Pulsejet

Being an internal combustion engine, three elements are required that must be supplied according to the operating cycle:

- Fuel
- Compressed air
- Ignition source

The correct way to use each one would be: turn on the ignition, inject the fuel and finally supply compressed air to the engine.

3.9.1 Fuel

As the morphology of the Pulsejet is very simple, it becomes a versatile engine for the use of fuels without finding notable differences. Thus, both liquid or gaseous fuels (LPG) and those of a solid nature such as coal are equally valid. During the experimental part, different types of fuel will be studied, assessing aspects such as cold start, storage size or their price.

If a historical overview of the fuels used since the start of operation of this type of engine is made, it should begin with acetylene (C_2H_2) used in the V-1. It is characterized by

being the simplest alkyne, highly flammable and capable of producing one of the highest adiabatic flame temperatures. However, the need to place a wooden or cardboard deflector in the exhaust pipe to stop the diffusion of acetylene before ignition was complete caused its disuse.

The evolution in the use of fuels goes hand in hand with the sizing of the engine. For larger engines, kerosene is interesting due to its operating cost. The problem with this type of propellant lies in the difficulty of starting the thermodynamic cycle at low temperatures. Therefore, it is advisable to start the cycle with a more flammable fuel such as propane (C_3H_8) to raise the internal temperature and then switch to a diesel or kerosene system.

For smaller engines, the following liquid fuels stand out: gasoline, methanol (CH_3OH), nitromethane (CH_3NO_2) and hydrogen (H_2). The most common is gasoline as it has a strict flammability index; extinguishing the flame if there is a mixture that is too rich or poor in oxygen favors intermittent combustion. On the other hand, both methanol and nitromethane have very high flammability rates, making their use dangerous and costly. Finally, due to its high calorific power, hydrogen burns at excessively high temperature, with a very short burning time.

Gaseous fuels or volatile gases do not require a fuel pump unlike liquids. The gas is introduced at a certain pressure in the tank. In addition, the boiling point of the gases used is much lower than room temperature, thus eliminating the need to vaporize. Some examples are methane (CH_4), butane (C_4H_{10}), or propane (C_3H_8).

3.9.2 Compressed Air

In order to produce any combustion process, the addition of an oxidant such as air is necessary. Said oxidant is normally at a pressure greater than atmospheric. If the amount of air is insufficient or the pressure is too low, it results in an air-fuel mixture that is too rich, causing combustion that is unable to produce the pulsating effect. The addition of compressed air is only necessary when starting the engine. Once the self-sustaining pulsating effect has been achieved, the presence of the fuel is enough for the correct functioning of the thermodynamic cycle.

3.9.3 Source of Ignition

There are different ways to ignite the air-fuel mixture. The simplest method is to place an exposed flame at the end of the propulsive duct (not very effective). The most widespread way is the use of a spark plug installed in the wall of the combustion chamber. With the help of a printed circuit board (PCB) or simply with a battery, a capacitor, a coil, platinum contacts and the spark plug itself, the electric discharge can be produced. Finally, there is the possibility of using a piezoelectric cell that must be repeatedly pressed to start the engine. The ignition source acts like the injection of compressed air only when starting the engine. This being unnecessary when stable operation is achieved as the residual gases from combustion are responsible for the repetition of the thermodynamic cycle.

3.10 Pulsejet relative to other Propulsive Systems

If it were necessary to define what distinguishes the Pulsejet engine from the rest of the engines present in current aviation. It would be about simplicity. Its easy construction, as it hardly has internal moving parts or simply does not have them, making its maintenance inexpensive. Due to its simple structure, the characteristic deflagration of this type of engine makes it a very inefficient option. The versatility of the Pulsejet engine in relation to the use of different fuels is another positive quality, most propulsive systems have a characteristic type of fuel. Finally, the low weight and production price have made the Pulsejet engine an object of research in the drone and light military aircraft market.

On the other hand, there are numerous technical limitations that compromise its use in the aerospace sector. Noise pollution as well as vibrations as a direct consequence of the pulsating effect are some of them. It also has a high specific fuel consumption (TSFC) compared to other types of engines. This is followed by a noticeable loss of energy in its thermodynamic cycle in the form of heat from the intake and exhaust ducts. It translates into a high fuel consumption value compared to turbofan type engines (they are the most used in current civil aviation).

The low compression ratios of the Pulsejet engine explain its poor thermodynamic efficiency. The compression of the air-fuel mixture is very low as the engine does not have any rotary compressor or piston that favors this compression. In a Pulsejet, the compression of the mixture is due to the displacement of the column of hot gases from the exhaust duct against the fresh air incoming from the admission one. This is a primitive form that barely manages to reduce the useful volume, harming the thermodynamic efficiency compared to alternative engines or turbofans.

Finally, although the cost of maintenance is relatively simple, valved Pulsejets are highly susceptible to mechanical breakage. The continuous exposure of these parts to fatigue during combustion means that their useful life is reduced and routine inspections are required.

3.11 Improving the Performance of a Pulsejet

The ability of the Pulsejet engine to have self-sustaining combustion for a longer time implies the need for research and improvement. The present study focuses on two objectives: to improve the combustion process and the durability of the moving parts of the Pulsejet engine.

Fuel injection into the combustion chamber wastes energy for the engine. As fuel is injected, some of it is released through the exhaust nozzle without actually being burned. For this reason, Simpson suggests placing a reed valve at the end of the injection tube. Thus, it is achieved that the greatest discharge of fuel occurs in the period in which the internal pressure of the combustion chamber is minimum. In this way, the total burning of the mixture is ensured by exerting a force on the blade that obstructs the hole through which the fuel is injected (*Figure 3.15*). As the thermodynamic cycle follows, the low pressure after the pulsing effect unclogs the injector, resuming fuel flow for cycle repetition.



Figure 3.15: Intermittent fuel injection mechanism [6]

As with fuel that does not participate in combustion, the intake air mass flow rate is also not fully involved. Some simulations carried out with Zheng reveal that placing an obstruction inside the combustion chamber increases the vorticity of the flow. In this way, the residence time of the air sucked into the chamber is increased, forcing it to participate in the combustion process. The correct proportion of air in combustion favors the thrust produced and reduces energy losses.

Regarding the durability of the valves that govern the intake in Pulsejet engines, there are possible improvements. Most valves used (*Figure 3.16*) today are very stiff and have a very high natural frequency; being a drawback as the vibrations produced are high.

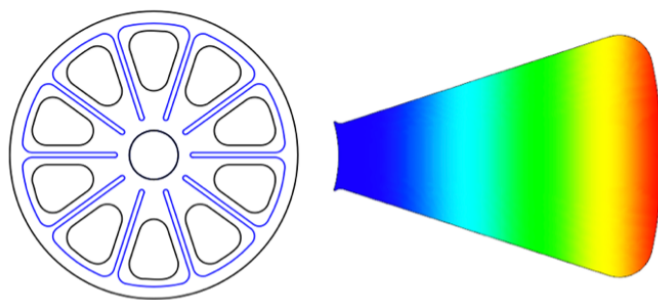


Figure 3.16: Conventional intake valve geometry and first mode of vibration [6]

Simulations carried out by Marisa Neuenburg and Daniel Ruiz from the Propulsion Department of CITEDEF suggest two new types of geometry for the intake valve that manage to dampen the first mode of vibration and reduce the natural frequency of the valve (*Figures 3.17 - 3.18*).

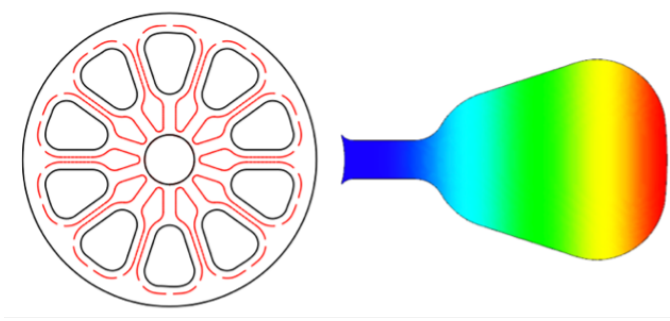


Figure 3.17: Prototype improvement valve I [6]

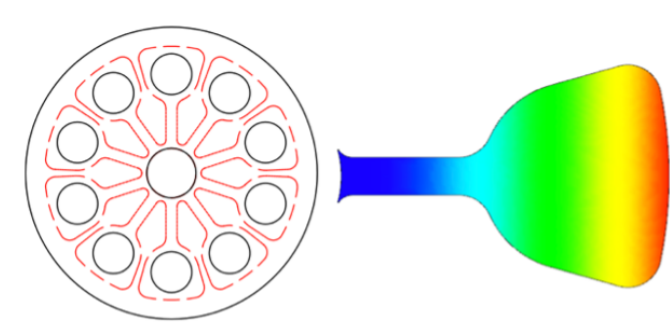


Figure 3.18: Prototype improvement valve II [6]

As explained in previous sections, there is an avant-garde technique that is still under study that significantly improves the performance of a Pulsejet engine. It is called PDE and it consists of making use of a pulsed detonation wave to ignite the air-fuel mixture. A considerable increase in internal pressure occurs when the fuel is detonated, increasing the rate of combustion of the mixture to speeds that exceed the speed of sound.

The need to increase the thrust produced by Pulsejet engines suggests the use of thrust augmentators at the ends of the engine. The function of these resembles an afterburner on a turbojet. The thrust force is calculated as the product of the amount of mass by the acceleration that is transmitted to it. The function of the thrust augmentator is to make use of Bernoulli's Principle and add air to increase the mass flow ejected. When another flow (cold air in this case) is added to a high speed flow, it results in a decrease in pressure. Consequently, the hot air expelled at high speed from the exhaust nozzle will be at a pressure lower than atmospheric. In this way, the flow is directed from the high pressure zones to the low pressure zones, simultaneously admitting cold outside air through the opening between the diffuser and the exhaust, which will subsequently be heated. By doing this, the sucked air expands, not affecting the final exit speed of the flow. In practice, these devices can only be used at low flight speeds, since, at high speeds, the drag produced does not compensate for the gain in thrust. The following image reflects the aforementioned improvement proposal (*Figure 3.19*).

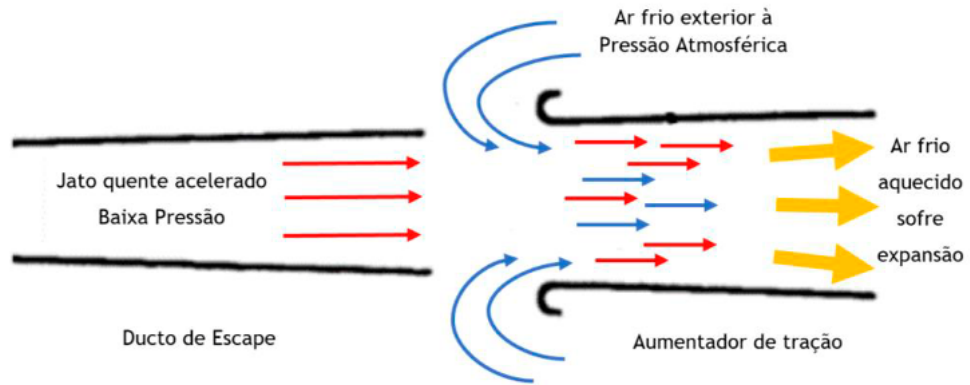


Figure 3.19: Thrust augmentator operating principle [3]

Chapter 4

Manufacture of the Pulsejet Engine

During the development of this chapter, all the phases followed for the final manufacture of the Pulse jet will be specified. It will start with the engine design drawings. It will be followed by the configuration of the test bench and the auxiliary systems that allow the operation of the engine and that have been used throughout the process. Finally, the manufacturing process followed in the UBI workshop will be described, as well as the acquisition of materials and the changes made with respect to the initial design.

4.1 Initial Pulsejet SetUp

The basis of the research aims to improve and add solutions to the difficulties encountered by a project carried out by a student from the Department of Aerospace Sciences at UBI [3]. Said study shares with this the engine that is going to be built; being a Chinese type valveless pulse jet engine.

One of the main design problems is the difficulty of finding a substantiated design theory. For this reason, the way in which it has been proceeded consists of following a calculation routine based on already existing engines together with equations from the literature. Unlike the previously carried out project, it has been decided to select a lower value for the diameter of the exhaust duct. This translates into a severe reduction in the final size of the Pulse jet as this variable participates in most of the equations that define the other measurements of the engine. Although, the value has been chosen based on the standard steel profiles since this condition will be essential for its manufacture. The assigned value is 50 [mm]. Attached below is *Figure 4.1* that represents the 2D dimensioned sketch with the three views of the engine.

It should be noted that some of the dimensions in *Figure 4.1* have suffered alterations caused by welding processes or by the availability of materials from the steel industry. The changes made will be delved into in future sections.

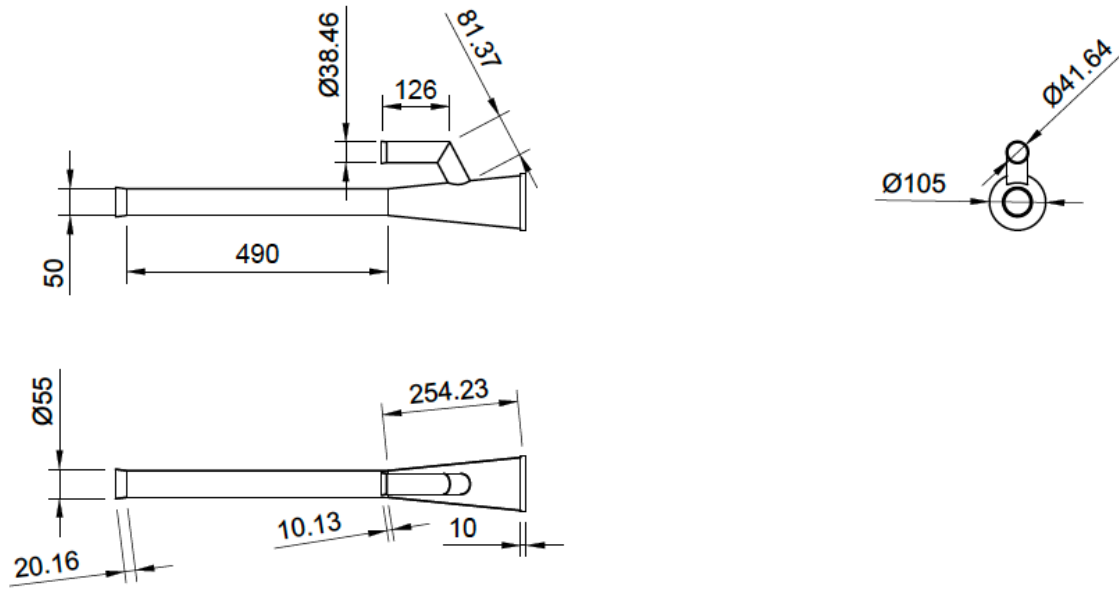


Figure 4.1: Initial dimensions of the Pulsejet

4.2 Manufacture of the Pulsejet

The first point to consider before starting manufacture is the selection of materials. Steel for wear resistance, toughness, machinability and hardness is the used material. Specifically, 304 series stainless steel. However, it is also crucial to select a suitable thickness as temperatures in the Pulsejet combustion chamber are above 1000 °C. In this way, to avoid the creation of cracks or distortions and to minimize thermal stresses on the motor walls, a minimum thickness of 2 [mm] has been taken throughout the assembly.

4.2.1 Admission

As a consequence of not having a machine capable of obtaining the desired diameter from a smooth steel plate, the steel industry has been resorted to. The tube has an external diameter of 38.5 [mm] and a bending machine has been used to obtain the final intake duct. The *Figure 4.2* shows the intake elbow already welded to the combustion chamber. Prior to this welding, the conduit has been cut at an angle close to 45° in order to be inserted; since the projection of the intake duct in the chamber is an ellipse.



Figure 4.2: Inlet Ducts

Regarding the angle selected in the intake elbow, an angle greater than 90° was required. The greater this angle, the smoother and more direct the entry of air and fuel into the engine will be, as there are no reductions in flow due to its passage.

4.2.2 Combustion Chamber

The same stainless steel plate used in the intake has been used for the construction of the combustion chamber. The first step has been to calculate the projection of the conic section to cut said surface with the help of a radial tool. Later, the optimal thing would have been to use a calender to obtain the conical shape. However, this machine was not existing in the UBI manufacturing laboratory. For this reason, it has been decided to place the metal plate in a cylindrical steel tube and obtain said geometry manually using a hammer. Next, the conical frustum has been welded. It should be said that this step has caused defects in the piece as the forming process has been carried out manually (see *Figure 4.3*).

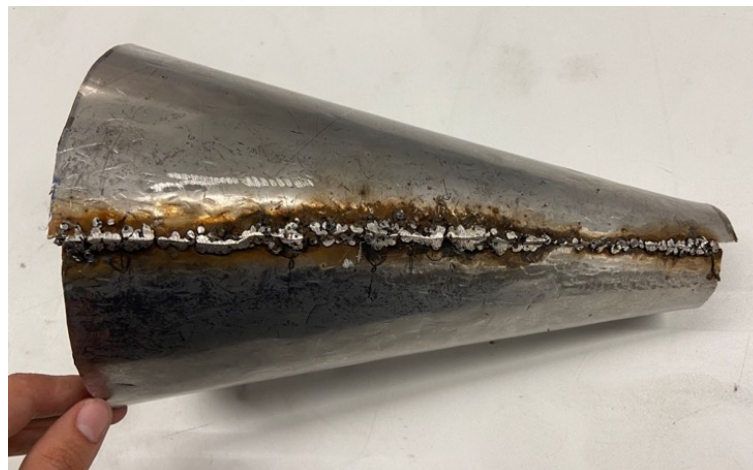


Figure 4.3: Combustion Chamber

Finally, a circular section of 105 [mm] of the same thickness has been cut and welded to the conical frustum. Additionally, a hole has been made to insert the intake duct. *Figure 4.3* presents the configuration of the combustion chamber.

4.2.3 Exhaust

As there is the same problem to obtain the cylindrical shape, the industry steel profiles have been used. Being a standardized diameter 50 [mm] it has been easy to obtain a 304 [mm] stainless steel conduit with the desired diameter. It has only been necessary to make a cut to obtain the designed length of 490 [mm]. Finally, the exhaust duct has been welded to the combustion chamber. The *Figure 4.4* shows the intake and exhaust ducts before being manipulated.



Figure 4.4: Intake and Exhaust ducts before being manipulated

4.3 Test Bench

The test bench used in the development of this work was carried out by a former student of the UBI [3]. Despite this, its configuration and layout is explained below.

When testing any type of static engine, it is necessary to have a structure with sufficiently rigid supports to guarantee safety during the test. The test bench was built from a set of 16x16 [mm] square section steel profiles welded by electric arc.

In addition to a rigid structure capable of withstanding vibrations, the test bench requires versatility in the coupling of the motor. Possible changes in the motor configuration or maintenance tasks require a quick decoupling. Two metal clamps with tightening screws around the exhaust duct were chosen.

Of the variables that are going to be measured, only one needs an element coupled to the test bench, thrust. Thus, two rails with bearings were installed on the seat to directly transmit the force to the load cell, which is connected to an Arduino board that transforms the information in order to allow its reading. These rails are made of plastic bearings,

which made it necessary to raise the Pulsejet 18 [cm] to increase heat dissipation to the environment. The high temperatures reached by the engine could differ in thrust value. In this way, a reliable value is transmitted through a steel cable to the load cell, which is not shown in *Figure 4.5*.

Finally, the test bench was fixed to the work table using three pressure clamps. These are not fixed and allow easy transport. The *Figure 4.5* represents the design made in CATIA V5R20 [3] with the final layout of the test bench.

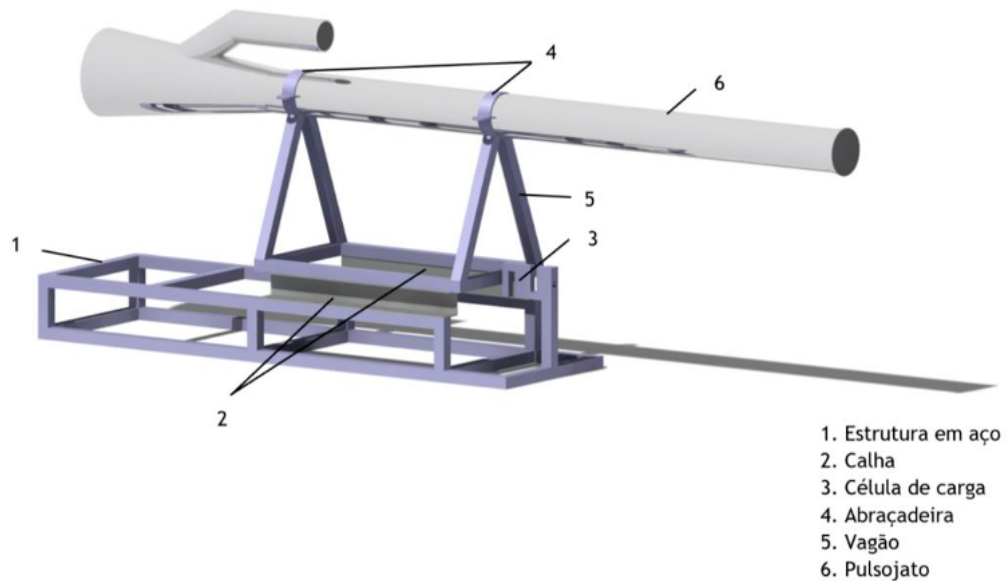


Figure 4.5: Pulsejet installed on the test bench [3]

4.4 Complementary Systems

There are three systems that without them the operation of the Pulsejet would not be possible: ignition system, fuel system and compressed air system. Once the ignition system is activated, the passage of fuel is allowed and the compressed air favors the diffusion of the mixture inside the combustion chamber and the initial cold ignition. Each of these systems is explained in detail below.

4.4.1 Ignition System

It is made up of a spark plug that discharges a high-voltage spark located in the combustion chamber that ignites the air-fuel mixture at the beginning of the operating cycle. The spark plug used is made up of a 20 [kV] ignition module with a discharge frequency of 16 [Hz], powered by a 3-cell lithium polymer battery with 11.1 [V] and 2100 [mAh] capacity. .

It is a NGK CMR6H spark plug that is commonly used in the automotive sector. Its coupling to the combustion chamber was installed in the form of a spherical cap fastened with a hexagonal metal nut in order to improve its support. After opening an M10x1 [mm] thread in the nut, it was welded to the circular wall of the combustion chamber. The ignition system used is shown in *Figure 4.6*.

When the ignition system is activated, an electric current of 20 [kV] flows through the positive terminal to the spark plug, causing an intermittent high-frequency spark. Meanwhile, the negative pole is connected to ground and is responsible for absorbing all the load. Once the Pulsejet reaches self-sustaining combustion, the ignition system is turned off by an operator.

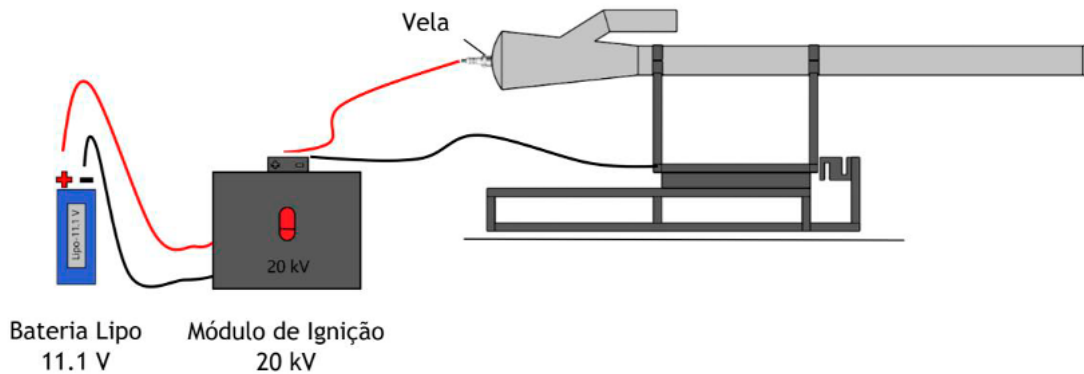


Figure 4.6: Ignition system [3]

4.4.2 Fuel Injection System

One of the most notable advantages of the Pulsejet is not being restricted to a specific type of fuel and can even operate with solid fuels (less volatile). Although, LPG fuel has been used since the use of liquid fuels implies a pre-vaporization before reaching the interior of the combustion chamber and a pressurization pump. Specifically, propane (C_3H_8) has been the selected fuel, after ruling out butane (C_4H_{10}) because it contains a lower specific heating value. In addition, the propane tank allows all the fuel it contains to be used, which does not happen with butane, which leaves a residual amount at the bottom.

The fuel injection system consists of a 9 [kg] propane tank at an average pressure of 9 [bar] at room temperature. The mass flow of injected fuel is controlled by an industrial reducer above the propane tank. When the fuel is reaching the combustion chamber there is a quick closing valve that cuts off the flow of fuel instantly.

Regarding the geometry of the injection system, it is an open tubular section that turned out to be the most effective configuration [3]. Both the injector and the fuel supply line are made of copper tube with an internal diameter of 4 [mm] with a melting point greater than 1000°C. After carrying out different experimental tests, it was concluded that the injector should be inserted 6 [cm] into the intake duct. A schematic of the fuel injection system is shown in *Figure 4.7*.

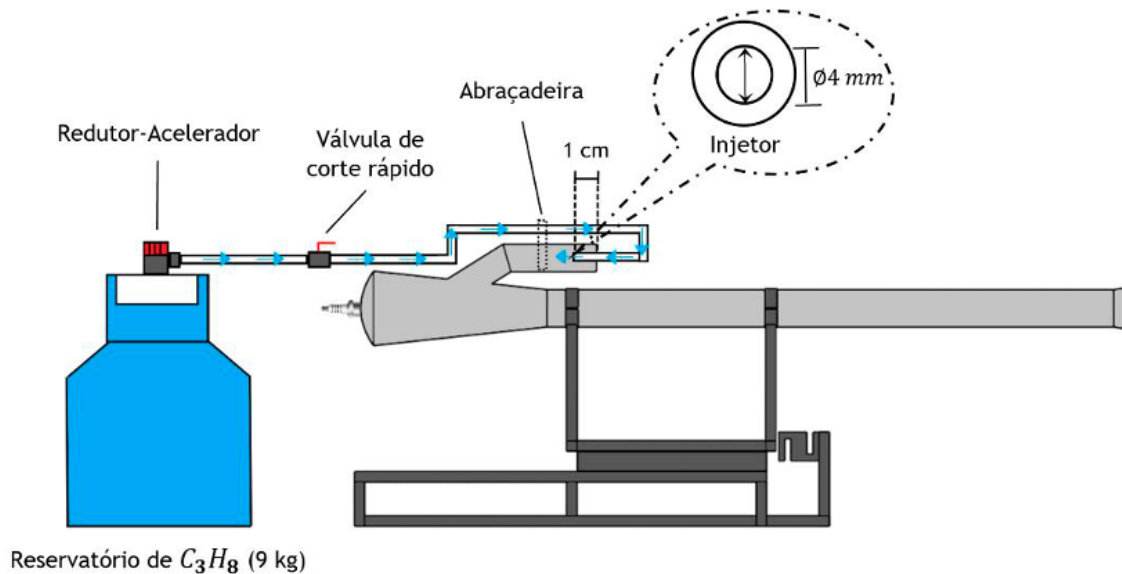


Figure 4.7: Fuel injection system [3]

4.4.3 Compressed Air System

This system is not strictly necessary but it is very beneficial for the correct operation of the engine. When starting the Pulsejet, air is injected with a higher pressure than ambient to trigger the deflagration in the combustion chamber. The compressed air system is a compressed-air gun installed in the UBI Aeronautical Engineering laboratory that is capable of regulating the pressure of the air thrown to the engine. When combustion is self-sustaining, air is no longer injected as the intake duct itself is responsible for the partial vacuum of high-speed combustion products.

4.5 Operational Problems

As it is an engine with such a simple configuration, it is vulnerable to operating damage. The dimensioning or the manufacturing process itself have derived the problems that are explained below. Hand in hand, the solutions implemented to solve these problems are described.

4.5.1 Ignition

Since an ignition system had already been used previously [3], a unipolar CMR6H NGK spark plug was used directly. There weren't too many problems with the ignition as it worked correctly in the already performed project. It is true that the neutral electrode had to be moved away from the central electrode, in order to cause a longer electric spark and thus achieve the Pulsejet's ignition more quickly.

4.5.2 Self-Sustaining Pulsing Effect

This turned out to be the biggest difficulty of the whole project. Being able to operate the Pulsejet without the external supply of compressed air. The different parameters were analyzed to try to locate a possible solution. Although, making use of the experience granted by the thesis carried out years ago [3], two factors were directly supported.

The first of these consisted of lengthening the exhaust duct by 1/3 of the total length of the Pulsejet, as the empirical experience has previously let known. That is, a 25 [cm] profile was cut and welded to the existing exhaust duct. The second was to add a divergent nozzle at the end of the exhaust and intake ducts. It was found that without this auxiliary complement it was not possible to achieve the self-sustaining effect. Once these changes were made, it was tested again and in just 30 [s] said effect was successfully achieved.

4.5.3 Constant Thrust

Once the problem of self-sustaining combustion was solved, an operating problem continued: when the fuel flow was increased, its operation was immediately interrupted. This can be explained because as the amount of fuel increased, the engine could not draw in a proportional amount of air to maintain the stoichiometric condition.

The solution was to install a convergence to the intake duct in order to promote a higher pressure differential. Thus, the absorption of air through the intake duct was favored. It turned out to be a success and it was possible to modify the flow of fuel injected into the engine for future tests.

4.5.4 Fuel

Initially, the goal of the project was to test a gasoline-powered Pulsejet engine. On the other hand, to use this type of fuel requires a more complicated ignition system that with the limited time it was not feasible to do. Liquid fuels are less volatile than gaseous fuels, which makes initial ignition difficult. Finally, propane gas has been used as explained in section 4.4.2 in the same way as the previous Pulsejet project [3].

4.6 Final Pulsejet SetUp

Taking into account the difficulties described above, the initial design of the Pulsejet has changed after the manufacturing process. The main reason for these changes has been the time to carry out the project. The fact that this work has been carried out in Portugal in the ERASMUS modality has meant shortening and intensifying the work deadlines defined at the beginning of the project.

As for the dimensioning of the motor, it has hardly undergone changes. Although, the intake duct had been designed to be bent and is finally made up of two pieces welded at an angle of 15° that form an angle with respect to the horizontal of 150°.

At the beginning, neither the intake duct nor the exhaust duct had a nozzle. After carrying out several tests that did not lead to the self-sustaining effect, it was needed to include the nozzles. As expected, the presence of this component improves thrust and TSFC values. However, time constraints and the need to manually build the nozzle (it has a conical section) without having a calender have contributed to dispensing with its use. Despite everything, the exhaust duct is still 490 [mm] long.

Chapter 5

Experimental Tests and Results

During this chapter, both the data acquisition process and the analysis of the results derived from said static test will be detailed. Both the morphology of the sensors used and the measurement techniques and the necessary programs to interpret them will be described.

5.1 Data Acquisition Instruments

In order to know the physical properties of the valveless Pulsejet, a series of tests were carried out as a function of time. Said properties are: thrust, combustion chamber temperature, specific fuel consumption (TSFC) and sound pressure level. To do this, a series of sensors located in the previously defined test bench were used, connected to a Mega 2560 board of the Arduino commercial software. The programming code is attached in the annex *Appendix A*. Next, the sensors used and the reason for their location are defined.

5.1.1 Temperature

There are different types of sensors capable of measuring temperature. The objective was to measure the temperature in the combustion chamber, so an “S” type thermocouple was chosen. This type of sensor, unlike others such as the “K” type, has a range between [-40, 1760] °C.

It was installed by extracting from the already completed Pulsejet project [3] the tube through which the two sensor terminals pass. Subsequently, said tube was cut using a radial tool, a spherical cap with a thread was added and welded 2 [cm] below the spark plug. In turn, a MAX31856 transformer was responsible for digitizing the signal from the thermocouple to the Arduino board. The *Figure 5.1* shows the thermocouple with its corresponding spherical cap already installed on the Pulsejet.



Figure 5.1: Thermocouple installed on the Pulsejet

5.1.2 Thrust

The way to measure the thrust in a static test involves the installation of a DYLY-103 type “S” load cell fixed to the structure of the test bench (see *Figure 5.2*). This type of sensor is made up of a steel cable that when the Pulsejet is turned on is stretched in the opposite direction. The strain generated in the sensor material is measured and converted into an electrical signal using strain gauges.

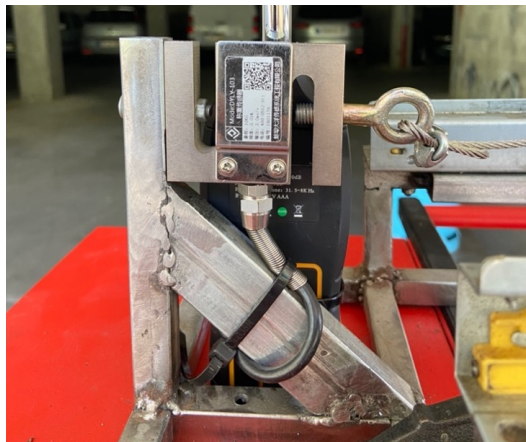


Figure 5.2: Load cell fixed to the test bench

On the other hand, as specified in the *Appendix A*, it was necessary to carry out a conversion from analog to digital signal. For this, an HX711 module was used.

5.1.3 Fuel Mass Flow

This type of variable was not measured with a conventional sensor. Basically, the change in mass of the propane tank over time was measured. To do this, a 16x16 [mm] steel scale was used that was already built in the UBI laboratory [3]. Said balance was connected to a load cell responsible for registering the mass variations. Specifically, it is a DYLY-103 “S” type cubicle, restricted to a maximum load of 20 [kg]. Said cell also made use of the HX711 module. The complete configuration of the scale was designed with CATIA V5R20 software by [3] as shown in *Figure 5.3*.

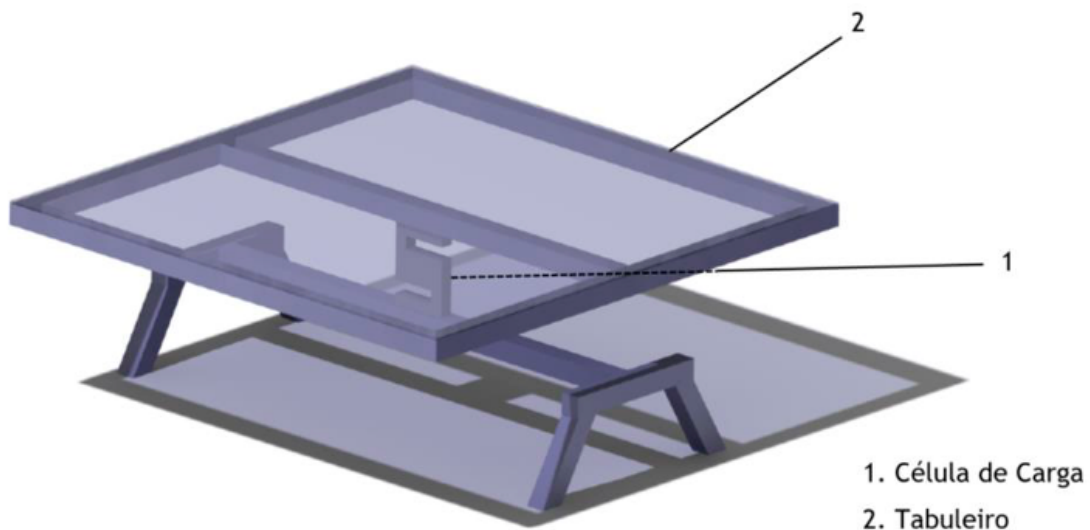


Figure 5.3: Platform for measuring the mass flow rate of fuel

In this way, the difference in the weight of the tank divided by the operating time made it possible to obtain the fuel mass flow rate.

5.1.4 Sound Pressure Level

One of the most noted drawbacks of the Pulsejet is the noise it generates. This makes it interesting to measure the sound pressure level in decibels [dB]. A SW-524 sound level meter connected to the Arduino board was used. The sound level meter has a measurement range between [30,130] with a tolerance of 1.5 [dB] and allows two types of weighting with respect to frequency: “A” or “C”. As what is sought is a curve independent of the frequency of the emitted sound, weighting type “C” has been used.

This sensor was placed at the outlet of the exhaust and intake ducts, respectively. Thus, it was possible to calculate the operating frequency following the method described in section 3.8 of this study. The *Figure 5.4* reflects the type of sound level meter used.



Figure 5.4: Sound level meter SW-524 [3]

5.2 Experimental Procedure for Data Acquisition

As in any test, it is necessary to define the conditions under which it will be carried out. As a consequence of not having a system capable of evacuating the exhaust gases, it was necessary to carry out the tests outside the UBI laboratory. In this way, the accumulation of flammable and harmful gases would not disturb the environment. The *Table 5.1* summarizes the environmental conditions on the day of the test.

Table 5.1: Environmental properties

Ambient Pressure	Ambient Temperature
1 [atm]	298 [K]

Before starting the ignition system, the pertinent security measures were guaranteed. Among them, check the tightness of the clamps that are responsible for fixing the engine to the test bench. Also, the use of protective thermal gloves, protection goggles and sound-insulating helmets; since the hearing can be damaged by noise pollution.

Once the security measures have been verified, the data acquisition proceeds as follows:

- Light the spark plug
- Inject the propane
- Introduce compressed air with the gun to facilitate initial ignition

In order to know the performance parameters of the Pulsejet, different tests were carried out with different mass flow rates of propane. For each flow rate, a value has been obtained

for: temperature in the combustion chamber, thrust force, mass flow of fuel delivered and sound pressure level.

Regarding the data acquisition method, there is a difference with respect to the project carried out in previous years [3]. In it, the sound pressure level was obtained directly with the Noise Meter dB software. Instead, in this project, all sensors including sound pressure have been connected to an Arduino Mega 2560 board (See *Appendix A*). With the programmed code, the measurements were read and stored at time intervals of 5 milliseconds.

Finally, to perform the data analysis and draw conclusions, the data from the sensor readings were exported to Microsoft Excel 2019. To do this, it was necessary to install a package called “Data Stream” available from Microsoft. The *Figure 5.5* clarifies the layout of the installed equipment around the Pulsejet and the test bench.

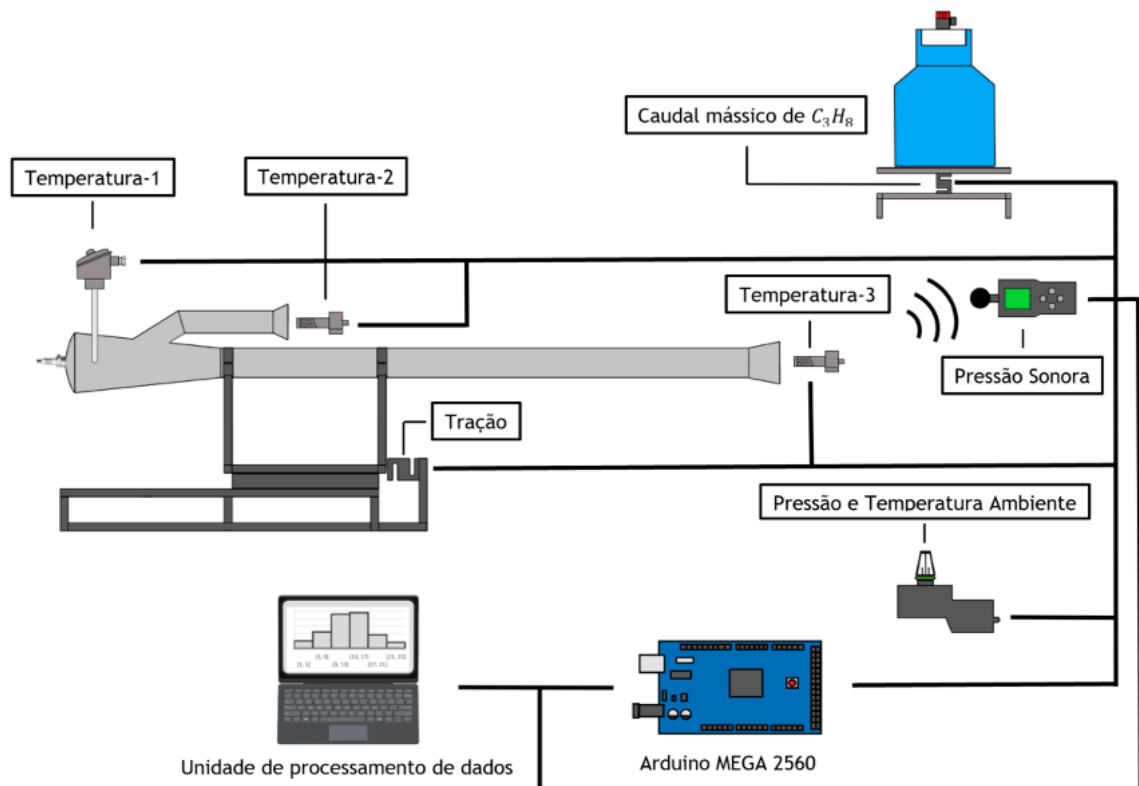


Figure 5.5: Experimental equipment for data acquisition [3]

5.3 Outcomes

During this section the results obtained during the test of the Pulsejet are presented. It is divided into subsections in order to analyze the most relevant parameters already explained in the theoretical foundations. It should be noted that the self-sustained combustion of the engine has been successfully obtained and that the fuel used has been propane.

5.3.1 Fuel Mass Flow

The amount of propane supplied to the Pulsejet was regulated through a reducer installed next to the propane tank. The way to quantify the fuel flow could be done using a scale that measured the initial weight (before starting the test) and the final weight of the tank. Thus, making the difference and dividing by the operating time, it was possible to know the amount of gas used per unit of time (see *Figure 5.2*).

Table 5.2: Fuel Mass Flow

Initial Weight	Final Weight	Operational Time	Mass Flow
14 [kg]	13.87 [kg]	200 [s]	0.65 [g/s]

During the engine test, variations were made in the injected fuel flow rate in order to obtain self-sustained combustion. Although, the results attached in [attach table] were obtained without changing the propane tank regulator for 200 [s].

5.3.2 Temperature

As for the temperature, it has not been possible to obtain the temperature inside the combustion chamber or the respective intake and exhaust ducts. As explained in section 5.1, an “S” type thermocouple was installed inside the combustion chamber. Before starting a new test, this gave consistent results close to 100 [°C] as a result of the previous test. However, as soon as the air gun was used, the cable stopped making contact and no value was acquired. It was tried to fix the two ends of the thermocouple with a copper cable and this caused an interference in the reading data. Attempts were made to change its position and conductivity was checked and no encouraging results were obtained.

Alternatively, a thermometer was used to try to approximate said temperatures. After ignition, already with self-sustained combustion, the intake duct showed temperatures close to 300 [°C]. This duct took time to reach this temperature as it was cooled by the injected compressed air necessary to start the engine. At the same time, the exhaust duct reached temperatures of around 400 [°C]. The problem with the combustion chamber was that the operating ranges of the thermometer were [-50, 550] [°C], so the display showed "maximum value". Being this value much higher than 550 [°C] as dictated by the literature and what was studied in previous sections; values between 1100 and 1400 [°C].

Unlike the Pulsejet built before [3], the combustion chamber was made of stainless steel, much more resistant than galvanized. Thus, it entered an incandescent state (See *Figure 5.6*) but which was controlled at all times and did not require it to be turned off.



Figure 5.6: Combustion chamber heating

5.3.3 Thrust

The load cell installed on the test bench was responsible for acquiring the thrust data. It was necessary to set a calibration value in the Arduino software (See *Appendix A*). During engine start-up, the readings were not constant and practically the cell did not have enough sensitivity to detect those values. Consequently, *Figure 5.7* plots thrust values as a function of time from the start of self-sustained combustion (this value being equal to 0).

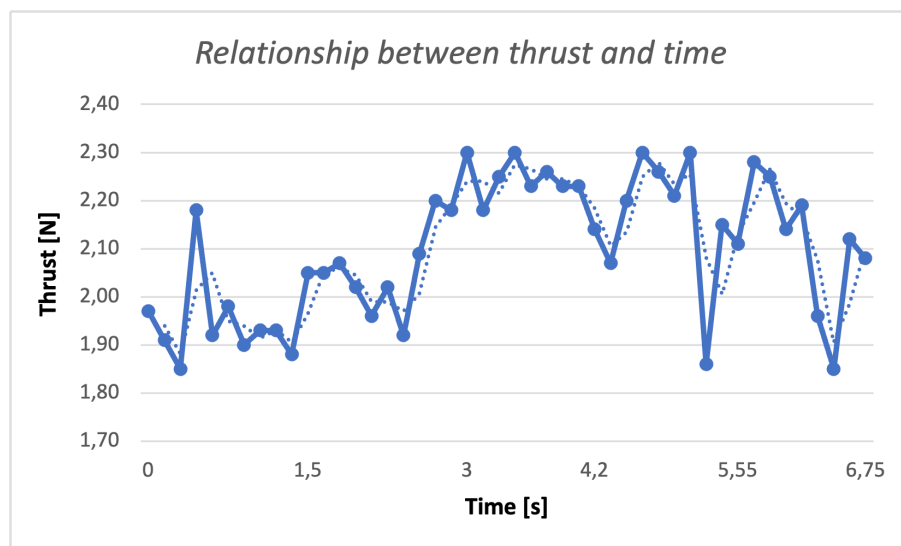


Figure 5.7: Relationship between thrust and time

During the tests carried out, the UBI laboratory technicians realized that the propane tank cylinder was near the end of its useful life. This translates into the impossibility of delivering a constant gas pressure. From the *Figure 5.7* it can be seen that the constructed valveless Pulsejet is capable of generating an average force of 2.1 [N].

Additionally, it was considered important to represent the thrust with variations in the flow rate of injected fuel. It should be noted that in order to maintain self-sustained combustion, the gas flow rate could not be increased by more than 4 [g/s] and that near this value there were operating problems. The data obtained is attached in *Figure 5.8*.

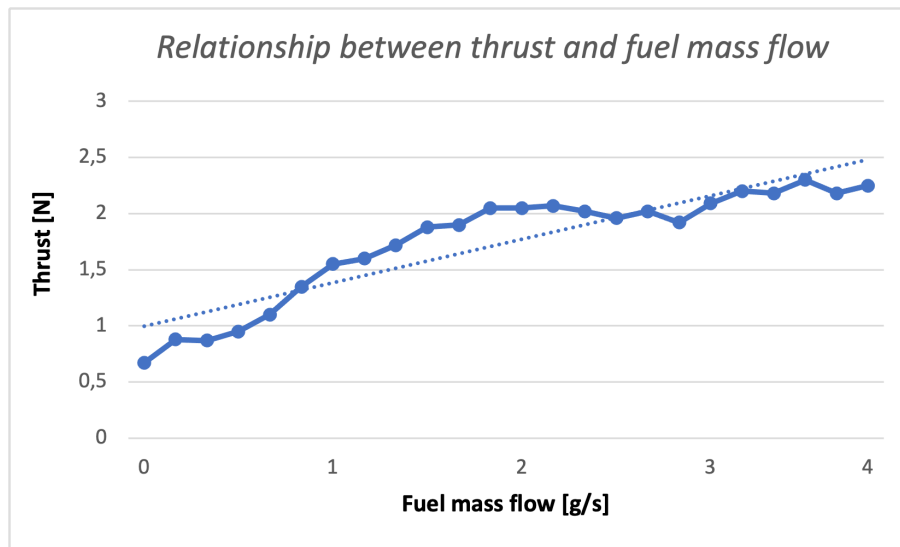


Figure 5.8: Relationship between thrust and fuel mass flow

As can be seen in *Figure 5.8*, an increase in fuel flow implies an increase in thrust as predicted by Melo [16] in numerical simulations. A linear trend line has been drawn that supports this statement. On the other hand, above 4 [g/s] the motor stopped working in a self-sustained way. It could be because there is an ideal ratio for the mixture of air and fuel. Above that value, the mixture is rich and has an excess of fuel that caused the inoperability of the Pulsejet. It is true that this fact is specific for this Pulsejet as it is present in the literature that this point was not reached until values close to 10 [g/s] of injected fuel flow for a Pulsejet of these dimensions. Despite the operational problem encountered, the conclusion is drawn that a Pulsejet engine can be accelerated with the increase in injected fuel. Up to 1.5 [N] increased thrust force for a 2 [g/s] increase in fuel flow.

Also, as it is an engine with pulse combustion, *Figure 5.9* shows the maximum thrust value recorded by the load cell. This value of 6.72 [N] is represented in yellow on the graph and is thought to be due to the previous heating of the Pulsejet as it was recorded in the last test carried out.

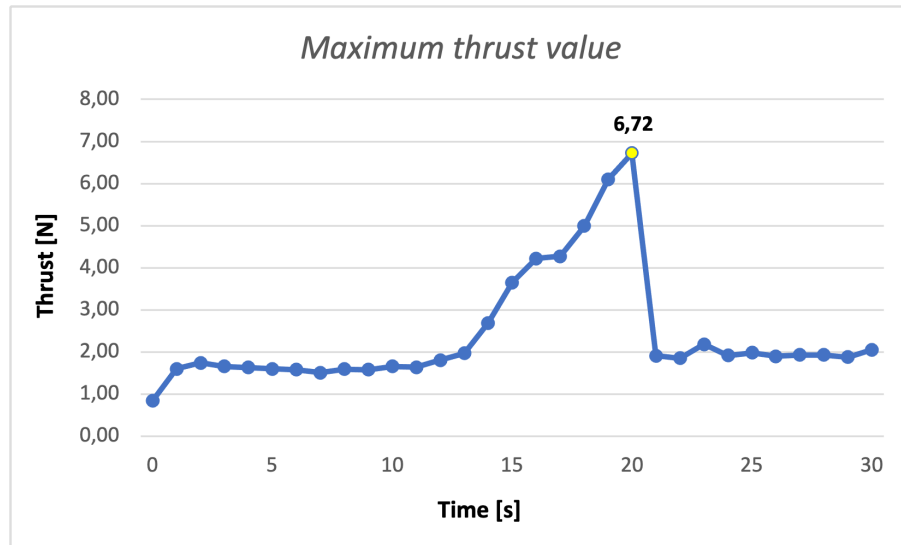


Figure 5.9: Maximum thrust value

5.3.4 Fuel Consumption

In order to better understand the amount of fuel consumed by the valveless Pulsejet, *Table 5.3* is presented. There, the specific fuel consumption is calculated for the different measured fuel flows.

Table 5.3: Thrust Specific Fuel Consumption of the Pulsejet

C_3H_8 Mass Flow [g/s]	Average Thrust [N]	TSFC [kg/(N h)]
0.5	1	1.8
1	1.6	2.25
2	2.1	3.42
3	2.3	4.7

The first conclusion drawn is that for lower flows of fuel injected, the engine burns the fuel that generates the thrust more efficiently. For higher flows, the efficiency tends to worsen and the specific fuel consumption as well. According to the literature, Melo [16] TSFC values obtained are lower than numerically predicted. Theoretically, to generate a thrust of 2 [N], 6 [g/s] of fuel flow would be needed. In practice, just 2 [g/s] is needed to generate such thrust. This means that the experimentally measured specific fuel consumption is up to 3 times lower than that required by the numerical study.

It must be said that the significant increase in fuel consumption is not equated with the increase in thrust obtained. That is, as the flow increases, fuel consumption increases more significantly than the thrust force.

5.3.5 Frequency

To collect the operating frequency of the valveless Pulsejet, the commercial software Audacity was used. However, after connecting the sound level meter as an audio input, it did not detect it. Consequently, using the laptop's microphone was tried, but the measurements were not consistent. As shown in *Annex A*, it can be seen that the relevant code was made in Arduino and was ready for measurement. Finally, due to time limitations and operational problems, it was not possible to obtain frequency values.

5.3.6 Sound Pressure Level

Sound pressure from the Pulsejet was collected using an SW-524 sound level meter installed downstream of the exhaust nozzle as shown in *Figure 5.10*.



Figure 5.10: SW-524

Additionally, different sound intensities were recorded depending on the flow of fuel injected. The *Figure 5.11* represents the distribution of sound intensity and the maximum intensity recorded.

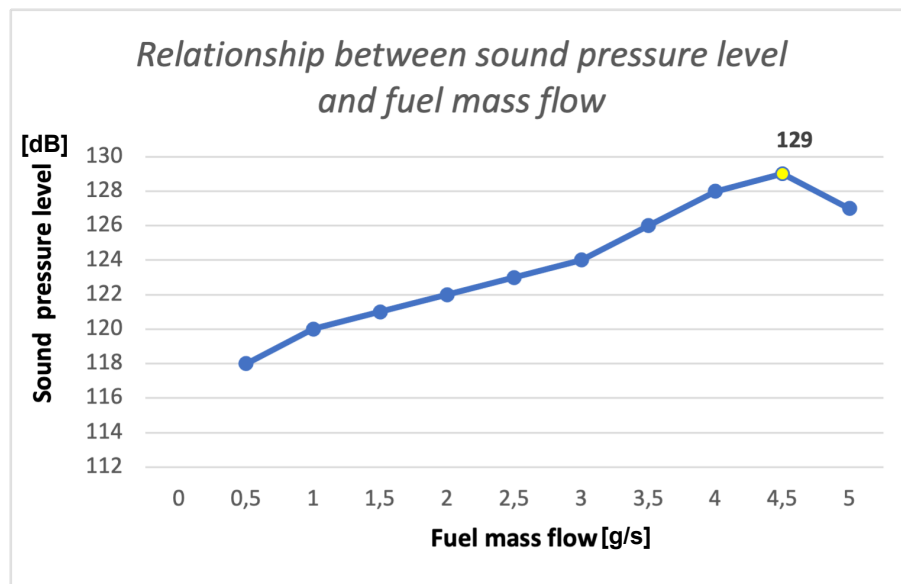


Figure 5.11: Relationship between sound pressure level and fuel mass flow

At first glance, no notable changes can be seen in the collected data. The cause of this may be due to interference in fuel injection pressure data. Despite this, it is seen from *Figure 5.11* that as the energy flow powering the Pulsejet increases so does the sound pressure. Thus, for flows close to 1 and 2 [g/s], values close to 122 [dB] are obtained compared to 128 [dB] recorded for higher flows. This more or less linear behaviour is observed until the engine reaches a value of 4 [g/s].

Chapter 6

Conclusions and Future Work

The development of this project allowed us to draw relevant conclusions regarding the Pulsejet without valves and its behavior. Thus, in this last chapter the conclusions of the experimental tests will be announced and which of the objectives set at the beginning of the thesis have been fulfilled and which have not. Finally, possible future research will be proposed that will allow a better understanding of this engine.

6.1 Conclusions

It is worth starting by saying that this project was born as a continuation of a numerical simulation [16] carried out at the UBI. Capturing that simulation and building a Chinese-type valveless Pulsejet engine was the first goal. After numerous sessions in the laboratory of aeronautical sciences of the UBI, this was achieved. Although, the real challenge was to get the self-sustaining speed of the engine. Firstly, a design was made in Autodesk following the proportions described in the literature. After making the first tests, it was seen that the motor did not achieve this effect if a continuous injection of compressed air was not made. To solve it and meet the main objective of the work, the length of the exhaust duct had to be increased by $1/3$.

There were other objectives such as the acquisition of data to compare them with the studies carried out in CFD [16]. Although many of them have been compiled and true conclusions have been drawn, other parameters such as the temperature in the combustion chamber or the frequency of operation due to operational problems have not been measured. Another objective that has not been fulfilled as expected has been to use different types of fuels for the subsequent comparison of parameters. The need to implement a more complex fuel injection system, since liquid and solid fuels are less volatile, could not be carried out due to time constraints.

Another existing difficulty during the development of the work has been the absence of machines capable of making profiles and conical shapes in the UBI workshops. To make the combustion chamber, it was necessary to manually shape the cone with a metal bar and a hammer. This led to numerous manufacturing errors such as the welding of the combustion chamber; It was not the perfect shape and it was difficult to close the stainless steel piece. Also the intake and exhaust nozzles were conical in shape. We proceeded by

cutting the existing nozzles of the Pulsejet manufactured years ago [3] and welding them to the new model. Regarding the manufacturing process, it is necessary to emphasize that there was not a steel profile bending machine either. To make the intake duct, the initial duct had to be cut at an angle of 75° to give it 150° with respect to the desired horizontal plane. Despite everything, both the laboratory technicians and the professor have successfully overcome the lack of machinery.

Experimental tests carried out lead to the conclusion that valveless Pulsejet engines are very susceptible to certain conditions. The first condition is the geometry of the engine, which must have the exact proportion between the exhaust and intake ducts in order to ensure that the shock waves released by each of them are synchronized. The second is the need to place the nozzle in the exhaust duct. Without it, it is not possible to achieve self-sustaining regimen. It is responsible for increasing the pressure differential, and thus promote the partial vacuum created inside the combustion chamber. The third condition is the placement of the injection duct at the engine intake. It cannot directly affect the combustion chamber or be too far from it. It was verified that at 4 [cm] from the beginning of the duct the thrust increased considerably.

Although the temperature of the combustion chamber could not be measured, a relevant fact was perceived during the tests. The more the temperature of the combustion chamber was increased, the sooner self-sustained combustion was achieved and, consequently, the thrust increased.

When the maximum thrust value of the engine was interpreted, two conclusions were obtained. The first is that the value of 6.72 [N] is lower than those cited in the literature and the one simulated in CFD [16]. The second one is that despite having this reduced value of maximum thrust, it would correspond to a higher fuel flow rate than that granted during the experimental test. This means that the experimentally measured specific fuel consumption is up to 3 times lower than that predicted by the numerical study.

The previous Pulsejet made at the UBI used 1.5 [mm] thick galvanized steel as material for the combustion chamber. Said material could not withstand temperatures close to 1400 [°C] and to maintain the safety and integrity of the engine they had to stop the tests. This time, 2 [mm] thick stainless steel was used for the construction of the Pulsejet. There were no punctures or cracks or laminations. The chosen material and its corresponding thickness were correctly selected.

6.2 Future Work

The approach of this type of engine with another type of fuel is very interesting. The problems due to the loss of pressure of LPG fuels make it difficult to obtain constant values. The fact of including an injection pump as an additional system, as would be done with liquid fuels, would allow a constant injection pressure to be maintained throughout the tests. Likewise, the improvement of the engine performance values (lowering the TSFC) and increasing the thrust values until they are as close as possible to what is cited in the literature are put on the table.

It is of interest to analyze the ways in which the thrust can be increased considerably. The

addition of thrust augmentators at the ends of the exhaust and intake ducts could be an effective solution such as Lockwood Hiller did [17]. Another possible investigation would be the use of a larger diameter fuel injector. Thus, the amount of fuel injected would be greater and the thrust values need to be analyzed.

Lastly, it would be fascinating to see the actual usefulness of this type of engine. Being able to introduce it in an aircraft structure such as a small plane or a drone and seeing the real performance under given flight conditions would allow us to know in a much deeper way why there is a limitation in aviation with this type of engine.

Appendix A

```
#include "HX711.h"
#include <Adafruit_MAX31856.h>

// Thermocouple S
Adafruit_MAX31856 max = Adafruit_MAX31856(33, 39, 35, 37);

// Loadcells
HX711 scale_1;
HX711 scale_2;
float reading_1;
float reading_2;
float reading_2_kg;
const int LOADCELL_DOUT_PIN_1 = 3;
const int LOADCELL_SCK_PIN_1 = 2;
const int LOADCELL_DOUT_PIN_2 = 5;
const int LOADCELL_SCK_PIN_2 = 4;
float Calibration1 = 431;
float Calibration2 = 218.5;
float thermo_cb;
float thermo_amb;
int mic;
int db;
float traction;
float dbvolt;

void setup() {
// Loadcells
scale_1.begin(LOADCELL_DOUT_PIN_1, LOADCELL_SCK_PIN_1);
scale_2.begin(LOADCELL_DOUT_PIN_2, LOADCELL_SCK_PIN_2);
scale_1.tare();
scale_2.tare();
scale_1.set_scale(Calibration1);
scale_2.set_scale(Calibration2);
Serial.begin(9600);
```

```
// Thermocouple S
max.begin();
max.setThermocoupleType(MAX31856_TCTYPE_S);
}
```

```
void loop() {
  TRACTION();
  FF();
  SOUND();
  TEMP();
  SERIALCOM();
}
```

```
void TRACTION() {
  reading_1 = scale_1.get_units();
  traction = reading_1 * 0.001 * 9.81 * (-1);
}
```

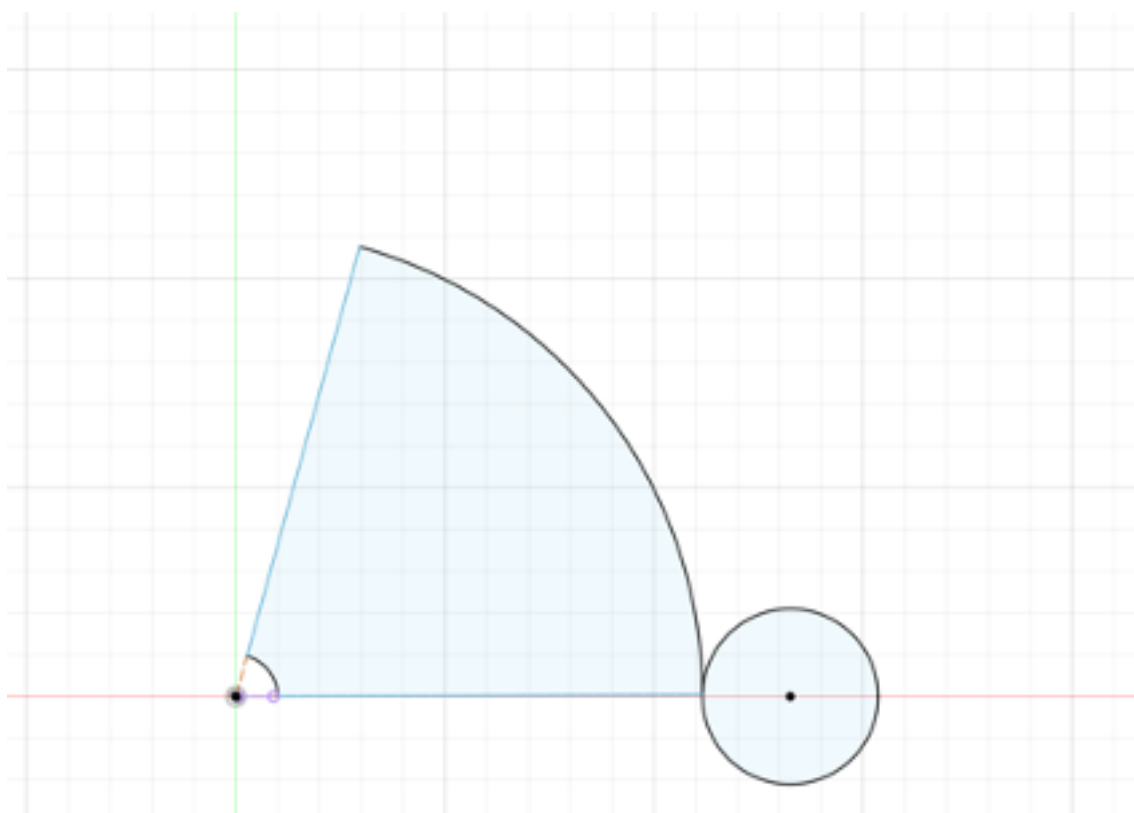
```
void FF() {
  reading_2 = scale_2.get_units();
  reading_2_kg = reading_2 * 0.001;
}
```

```
void SOUND() {
  int mic = analogRead(A2);
  db = 20*log10(mic);
  dbvolt = (5/1023) * mic;
}
```

```
void TEMP() {
  thermo_cb = max.readThermocoupleTemperature();
  thermo_amb = max.readCJTemperature();
}
```

```
void SERIALCOM() {
  Serial.print(traction);
  Serial.print(",");
  Serial.print(reading_2_kg);
  Serial.print(",");
  Serial.print(thermo_cb);
  Serial.print(",");
  Serial.println(thermo_amb);
}
```

Appendix B



Bibliography

- [1] FiddlersGreen. *The WWII V-1 Doodle Bug Flying bomb*, www.fiddlersgreen.net/models/Aircraft/V1.
- [2] B. Ogorelec. Valveless pulsejet engines 1.5.
- [3] Miguel Ângelo Lopes Duarte. Construção e ensaio estático de um pulsojato sem válvulas.
- [4] A. P. Kiker A. V. Kuznetsov W. L. Roberts T. Geng, F. Zheng. *Experimental and numerical investigation of an 8 cm valveless pulsejet*. 2007. Experimental Thermal and Fluid Science, nº 31, pp. 641-647.
- [5] A. F. El-Sayed. Aircraft propulsion and gas turbine engines. florida: Crc press, 2017.
- [6] B. Simpson. *The Valveless Pulse Jet*, <https://aardvark.co.nz/pjet/valveless.htm>, 13 of February, 2022.
- [7] S. S. Prasad e V. Krishna S. Kumar. *Desginf of a Pulsejet Engine for UAV*. International Jorunal of engineering Research and technology, 2014. vol III, nº 9, pp. 670-675.
- [8] Narayan. *Pulsejet Technology*. 2013.
- [9] A.F.El-Sayed. *Fundamentals of Aircraft and Rocket Propulsion*. Springer, 2016. Pulsejet, Ramjet, and Scramjet Engines, pp. 315-330.
- [10] C. Wenxiang Z. Tao, Z. Yong. *Numerical investigation of typiical valveless pulse combustor working process*. 2017. Energy Procedia, vol. 141, pp. 287-291.
- [11] K.T. Dougherty D.E. Paxson, J. Wilson. Unsteady ejector performance: An experimental investigation using a pulsejet driver. 38th aiaa/asme/sae/asee joint propulsion conference exhibit- indianapolis, 2022.
- [12] H. Miyanishi T. Setoguchi K. Kaneko T. Nakano, M. Zeutzius. *Studies on Pulsejet engine by wind tunnel testing*. 2001. International Journal of rotating machinery, vol. 7, nº 2, pp. 79-85.
- [13] J.C Pascoa F. Rodrigues M. Trancossi, O. Mohammedalamin. *Thermodynamic Analysis and Preliminary Design of the Cooling System of a Pulsejet for Aeronautic Propulsion*. 2016. INTERNATIONAL JOURNAL OF HEAT AND TECHNOLOGY, pp. 528-534.

- [14] M. L. Coleman. *OVERVIEW OF PULSE DETONATION PROPULSION TECHNOLOGY*. Columbia: CHEMICAL PROPULSION INFORMATION AGENCY, 2001.
- [15] C. Tharratt. *The propulsive Duct*. Aircraft Engineering and Aerospace Technology, 1965. vol. 37, nº 11, pp. 327-337.
- [16] A.S. M. Melo. *Pulsejet Engine Performance Estimation*. Dissertacao de mestrado, Dept. Ciências Aeroespaciais, Universidade da Beira Interior, Covilha, 2019.
- [17] J. E. Leckett R. M. Lockwood, E. R. Sargent. *THRUST AUGMENTED INTERMITTENT JEET LIFT-PROPULSION SYSTEM*. Bureau of Naval Weapons, Washington, 1960.